Numerical Analysis of Plate Fin Heat Exchanger at Cryogenic Conditions

A THESIS SUBMITTED IN PARTIAL FULFILLMENT OF THE

REQUIREMENTS FOR THE DEGREE OF

Master of Technology

In

Mechanical Engineering

By

SANDEEP MUDGALA (213ME5451)

Mechanical Engineering Department

National Institute of Technology

Rourkela

2015

Numerical Analysis of Plate Fin Heat Exchanger at Cryogenic Conditions

A THESIS SUBMITTED IN PARTIAL FULFILLMENT OF THE REQUIREMENTS FOR THE DEGREE OF

Master of Technology
In
Mechanical Engineering

By

Sandeep Mudgala (213ME5451)

Under the guidance of

Prof. Ranjit Kumar Sahoo

Mechanical Engineering Department
National Institute of Technology
Rourkela
2015

National Institute of Technology
Rourkela

CERTIFICATE

This is to certify that the thesis entitled, "**Numerical Analysis of Plate Fin Heat Exchanger at Cryogenic Conditions**" submitted to **National Institute of Technology, Rourkela** by **Sandeep Mudgala,** Roll No**. 213ME5451** f**or** the award of the Degree of **Master of Technology** in **Mechanical Engineering** with specialization in**" Cryogenic and Vacuum Technology"** is a record of bonafide research work carried out by him under my supervision and guidance. The results presented in this thesis have not been, to the best of my knowledge, submitted to any other University/ Institute for the award of any degree or diploma.

The thesis, in my opinion, has reached the standards fulfilling the requirement for the award of degree of **Master of Technology** in accordance with regulations of the Institute.

Place: Rourkela

Date:

Prof. R.K Sahoo
Dept. of Mechanical Engineering,
National Institute of Technology
Rourkela-769008
Orissa

ACKNOWLEDGEMENT

I would like to express my greatest gratitude and respect to my supervisor **Prof. Ranjit Kumar Sahoo,** for his excellent guidance, valuable suggestions and endless support. He has not only been a wonderful supervisor but also a genuine person. I consider myself extremely lucky to be able to work under guidance of such a dynamic personality. Actually he is one of such genuine person for whom my words will not be enough to express.

I also express my special thanks to our research scholars **Mr.Ajay Kumar Gupta**, **Mr. Pankaj Kumar**, and my friend and classmate **Mitravanu Sahoo** for their support. It was impossible for me to complete my project without their help. I would like to express my thanks to all my classmates, all staffs and faculty members of mechanical engineering department for making my stay in N.I.T. Rourkela a pleasant and memorable experience and also giving me absolute working environment where I could use my potential .

Last but not the least; I want to convey my heartiest gratitude to my parents for their immeasurable love, support and encouragement.

Sandeep Mudgala
Roll no.: 213ME5451
Cryogenics and Vacuum Technology
Mechanical Engineering Department
National Institute of Technology

Date:

ABSTRACT

Compact heat exchangers, especially plate fin heat exchangers (PFHE) are playing an important role in various fields of science and technology. Especially in cryogenics with its high compactness providing very high degree of heat exchange area per unit volume (of the range of 1000m^2/m^3) and high effectiveness of 0.95 and above, PFHE is one of the most desirable equipment in the cryogenic field. Various forms of flow configurations and heat transfer surfaces for the PFHE have been studied and used. In this investigation PFHE of Aluminium alloy Al-3003 with rectangular offset-strip fin is simulated by the cold layer test method to find the effectiveness and pressure drop at low temperatures using liquid Nitrogen i.e. of the range of 80K-110K as the inlet temperature of the cold fluid and inlet of hot fluid at room temperature (taken to be at 315K). Simulated prediction is done using simulation software Aspen MUSE. The comparison between the cold layer test and hot layer test is done and their performance factors like effectiveness and pressure drop are compared. Results obtained from the simulation software Aspen MUSE show that at low temperatures a high effectiveness is displayed by the test PFHE with pressure drops under the prescribed limits. Also mass flow rate at which experimentation can be carried out is also found out.

Keywords: Plate fin heat exchanger (PFHE); offset-strip fins; Colburn factor; Friction factor; cold layer test

CONTENTS

List of Figures:

List of Tables:

NOMENCLATURE:

A_o	Total heat transfer surface area (m^2)
C	Heat capacity rate (J/sec-K)
C_p	Specific heat (J/kgK)
D_e	Equivalent Diameter (m)
f	Fanning friction factor (dimensionless)
G	Core mass velocity/flux (kg/m^2s)
h	Convective heat transfer coefficient (W/m^2 K)
j	The Colburn factor, (dimensionless)
K_f	Conductivity of the fin material (W/m- K)
$\dot{m}$	Mass flow rate (kg/sec).
NTU	Number of transfer units
P	Pressure (bar)
Re	Reynolds number
Re^*	Transient Reynolds number
T	Temperature of fluid (with subscripts c, h or i, o) (K)
U_o	Overall heat transfer coefficient (W/m^2 K)
ε	Effectiveness
η	Efficiency

Subscripts:

c	Cold fluid side
h	Hot fluid side
i	Inlet
o	Outlet
max	Maximum
min	Minimum
m	Mean
w	Properties at the wall temperature

CHAPTER-1

Introduction

1. INTRODUCTION

1.1. Compact Heat Exchanger:

With the increasing developments in the fields of science and technology the size of the equipments that are to be utilised are decreasing. One such occurrence is in the case of heat exchangers. As the need arises for increase in the performance factor as well as keeping the weight and volume of the heat exchanger strictly low, a new breed of heat exchangers emerged that were to be known as compact heat exchangers. These heat exchangers find application in industries like aircraft and cryogenics.

Technically, a heat exchanger with the heat transfer surface area per unit volume (β) greater than 700 m^2/m^3 is said to be a compact heat exchanger. Their increased surface area also works to counteract the low heat transfer coefficient associated with the gas flow during the gas-to-gas or the gas-to-liquid (liquid-to-gas) heat exchange for which compact heat exchangers are generally used for. The passages used in these exchangers are generally short and made of cross-sections of rectangular or triangular geometries with the inclusion also of circular tube or parallel plate channel. This enables a wide range of Prandtl numbers ranging from $0.1<Pr<\infty$ that gathers a wide range of fluids from gases to high viscous fluids. The most evident example being our lungs with 20000 m^2/m^3 of heat transfer surface density. Other examples are the regenerator of a Stirling engine (15000 m^2/m^3), glass ceramic gas turbine heat exchangers (6000 m^2/m^3), car radiators (1000 m^2/m^3), etc. The heat transfer surface density is given by;

$$\beta = \frac{heattransferarea}{heattransfervolume} = \frac{4\sigma}{D_h}$$

Where, $\sigma = 0.833$= Heat transfer surface density

D_h = Hydraulic Diameter (m)

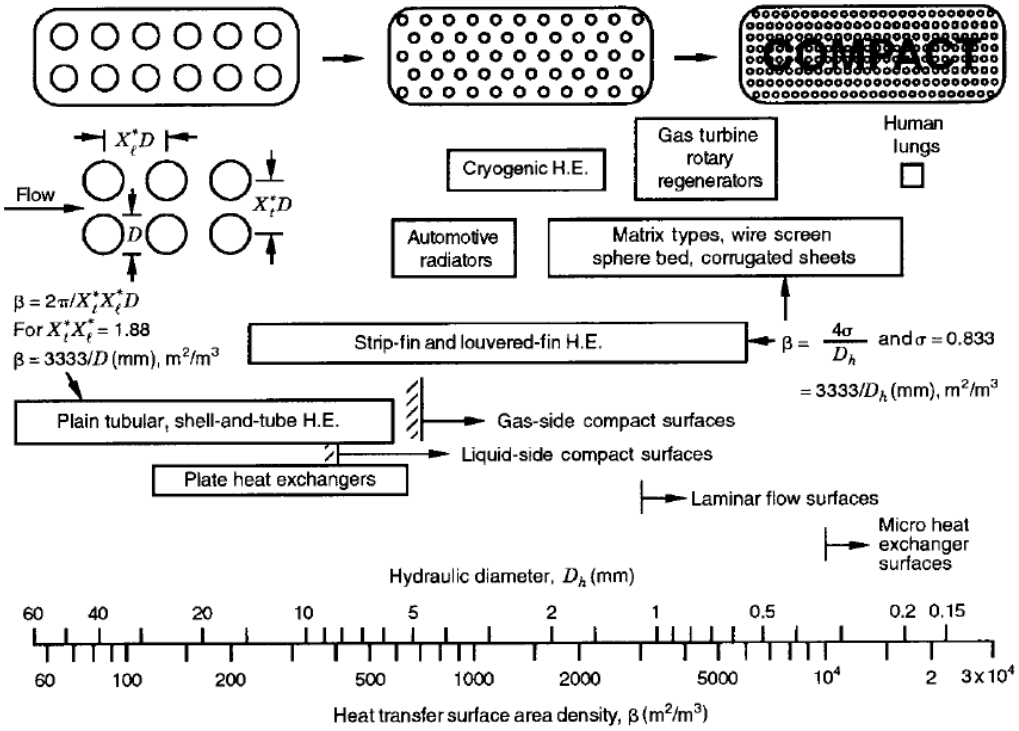

Figure.1.1 Heat exchange surface area density range of heat exchanger surfaces [2].

1.1.1 Types of Compact Heat Exchanger

1) Plate heat exchanger (PHE)

2) Plate fin heat exchanger (PFHE)

3) Printed circuit heat exchanger (PCHE)

4) The marbond heat exchanger

5) Ceramic heat exchanger

6) Spiral heat exchanger (SHE)

1.2.Plate Fin Heat Exchanger (PFHE):

Plate fin heat exchanger is a breed of compact heat exchanger that is constructed of stacked parallel flat metal plates and corrugated fins that are joined together by brazing technique to form a single block. The parallel stacked flat metal plates are known as the parting sheets and they act as the elementary heat exchange surfaces while the corrugated fins forms the secondary or collateral heat exchange surfaces.

The fluid flow and the heat transfer between the streams occurs in the passages formed between the parting sheets and the fins. There is also another metal plate known as the side bar that holds the parting sheet and fin construction so that:

- The streams exchanging heat do not come in direct contact with each other
- The fluids stay in their respective passages and not spill over.
- It acts as a linkage in the thermal circuit, with the fins and the parting sheet to provide rigidness and stability to the structure.

The first and the last metal flat sheets used in the heat exchanger are known as the cap sheets used to cover the brazed block. The thickness of the cap sheets is more than that of the parting sheets and its reason is the same as that with the side bars, i.e. , to provide support to the structure and also to sustain the high pressures that can be more than the atmosphere.

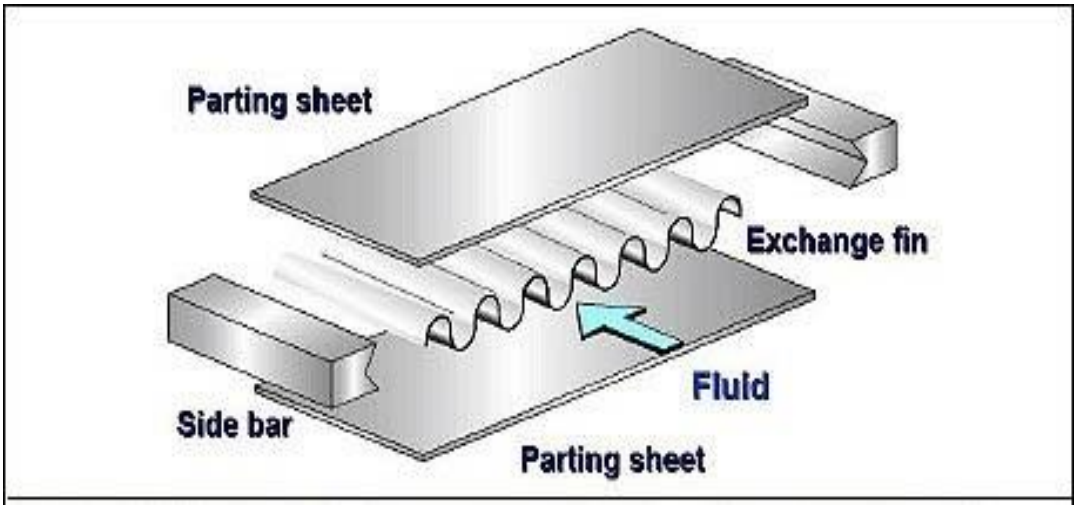

Figure 1.2 Detailed view of plate fin heat exchanger

1.2.1. Materials Used In Plate Fin Heat Exchanger:

Plate fin heat exchangers are usually manufactured from alloys of aluminium or stainless steel and the material of construction largely depends on the process temperature and conditions. Aluminium alloys are especially applicable for cryogenic applications due to their low load and low specific mass having brilliant ductility and greater strength under those conditions. The fins and the side bars are generally secured to the parting sheet by employing salt bath dip brazing or the current favourite, vacuum brazing technique. The filler used for Al brazing is an Al alloy only but having a lower melting point. For stainless steels, Ni alloy is used as brazing filler material.

1.2.2. Manufacturing Process:

The manufacturing technique for the plate fin heat exchanger for all size and shapes using different materials are basically the same. The assembly of an array of flat sheets and wrinkled fins in a sandwiched manner with the cap sheet at the top and bottom is the basic methodology of construction of the plate fin heat exchanger. This assembly is then stacked in alternate layers to form the required passages for the fluid flow. The entire stacked assembly consisting of the parting sheets, the corrugated fins, the side bars, the end plates and the cap sheets are then held in a jig that is set to a predesignated load and then planted in a furnace for brazing, which forms the exchanger unit.

Then comes the header containers and the nozzles through which the fluids enter and exit. These components are welded to the block with taking the utmost care so as to not disturb the brazed joints seating.

The common types of brazing process used are:

1. Salt bath brazing technique
2. Vacuum brazing technique

Salt bath brazing technique or salt bath dip brazing is a technique of brazing used to join metals by dipping the assembled block into a molten pool or bath of salt that is usually the fluorides or chlorides of the soluble base metals. The liquid salt bath is maintained at a temperature of 600°C .the stacked assembly of the components is preheated to about 500-550°C to ensure uniformity of temperatures across the block. As

the block is immersed in the molten salt the heat transfer takes place rapidly and the molten salt that acts as the flux comes in contact with the inside and outside surfaces almost simultaneously. The salt bath also ensures the removal of dirt and other sticky particles from the surface of the block. It also removes the detrimental aluminium oxide layer that forms due to oxidation on its surface thus protecting the joints.

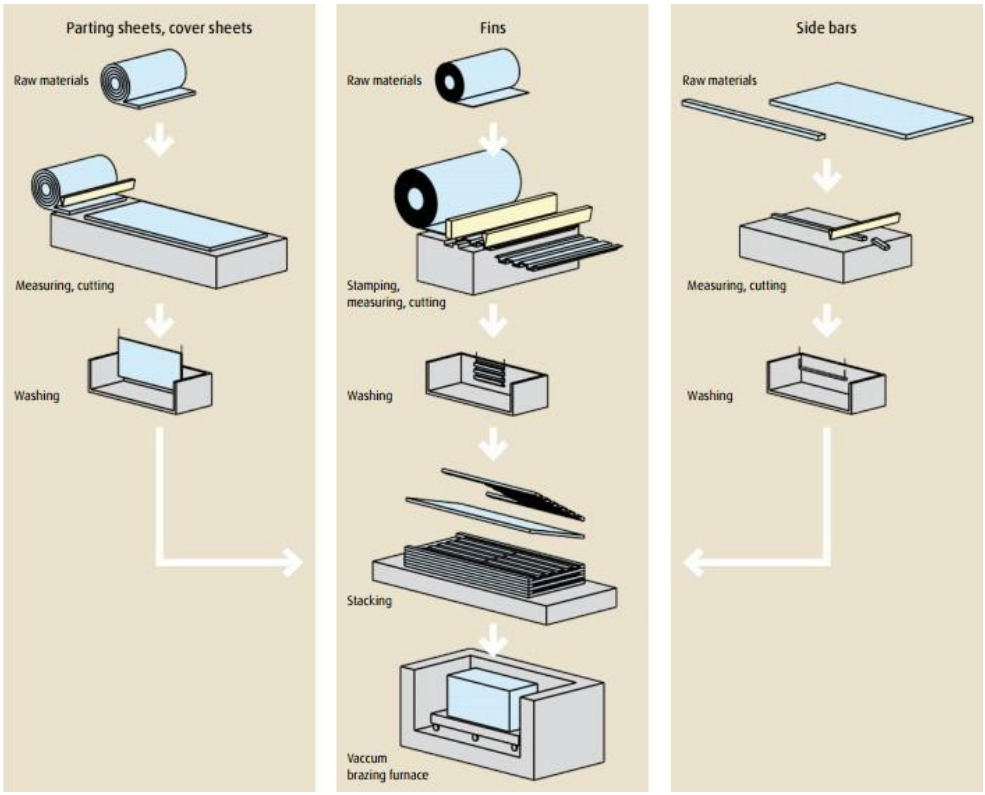

Figure 1.3 Manufacturing of plate fin heat exchanger components

The immersed block is brazed after which it is then removed and cleaned using water and is further dried.

In the Vacuum brazing technique, the most important point to remember is that there is absence of oxygen and hence the brazed joint is free from defects due to the oxides formed during oxidation. A high vacuum of about 10^{-6} – 10^{-8} millibar is maintained in the vacuum furnace so that an oxidation free environment can be achieved. In this process the block containing the assembled components is heated up to the temperature of the brazing filler metal through radiation and conduction. There is no pre-heating of the furnace nor is any type of flux required in this process. The evacuation and desorption of the gases results in a clean and ideal environment and there is no need for washing or pickling of the block.

Most heat exchanger metals such as aluminium and its alloys, stainless steel, nickel and copper alloys are brazed successfully using the vacuum brazing process.

1.2.3. Applications of Plate Fin Heat Exchanger:

Due to its high compactness and effectiveness it is used in a wide variety of fields and at a wide variety of temperature and pressure ranges. It can be used liquid-gas, gas-gas or multi-phase activities with the option of multi-streaming also. Plate fin heat exchangers find application in:

- Cryogenic Field: it is used in the segregation and liquefaction of air, natural gas, etc.
- Petrochemical production: like in the fractionation of LPG.
- Large refrigeration systems and air-conditioning systems
- Aerospace industry mainly in hydraulic oil and avionics cooling and fuel heating
- Automobile industry mostly for making high performance radiators
- Pollution control systems
- Fuel cells
- Fuel refining and modification plants
- Heat recovery plants

1.3.Flow Patterns:

In a plate fin heat exchanger the flow arrangement is a decisive point in the maximised heat transfer ability. Primarily, there are three flow patterns in a heat exchanger;

1. Parallel flow
2. Counter flow
3. Cross flow

The parallel flow arrangement is the simplest of the three but offers the lowest heat transfer rate or recovery, whereas the counter flow pattern gives the highest heat transfer rate. Intermediate between these two is the cross flow arrangement. The above three flow patterns are in a more theoretical sense but actual working systems are more complex and

to ensure the efficient working in the practical sense a combination of flow pattern is used. This gives rise to another type of flow arrangement known to be as the cross-counter flow arrangement. Thus in the practical world, the flow arrangements are classified as:

1.3.1. Cross flow:

In cross flow arrangement, the fluids (hot and cold) cross one another, usually in a direction perpendicular to each other. The fluid may be mixed or flowing separately in the passages while through the heat exchanger. In the case of mixed flow of the fluid, the temperature will be constant across any cross section and will differ only in the flow direction, whereas in the case of unmixed flow the temperature across the section is not uniform. Cross flow pattern should be chosen when the effectiveness requirement is not high or when one or both fluids are in isothermal condition. Examples are, automobile radiators, cooling units of refrigeration systems.

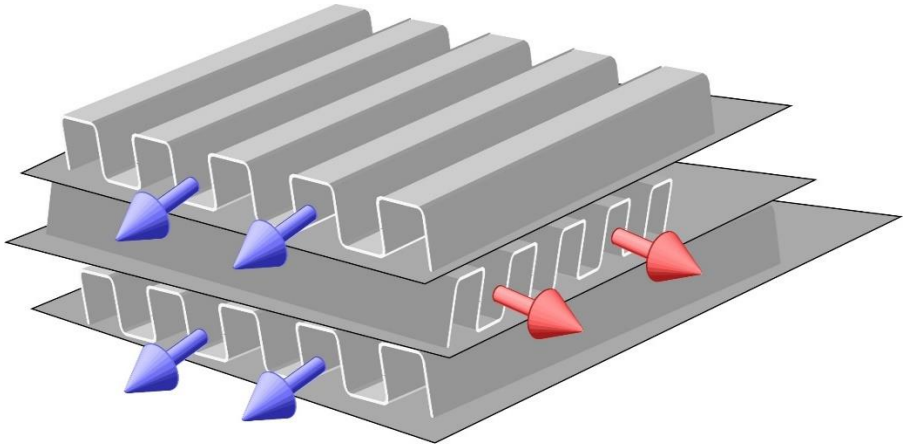

Figure 1.4 Cross flow pattern

1.3.2. Counter flow:

In this type of flow, the hot and cold fluids flow in opposite directions but in parallel to each other. The temperature difference between the two fluids remain more or less near constant. The counter flow provision gives the maximum rate of heat transfer for a specified surface area. Thus it makes these heat exchangers the most preferred ones for the efficient heat exchange in fluids. Exclusive usage is evident in the field of cryogenics for liquefaction and process plants.

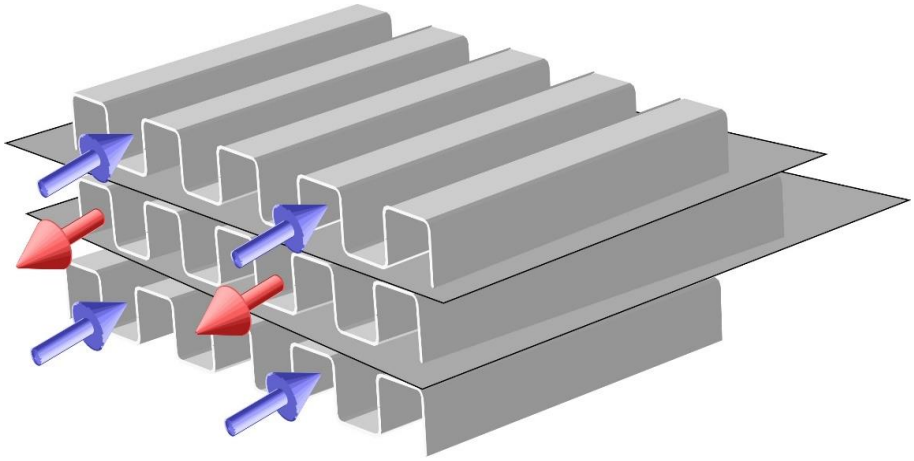

Figure 1.5 Counter flow pattern

1.3.3. Cross-counter flow:

This type of flow pattern is the combination of counter and cross flow alignments utilising the high thermic performance of counter flow and the greater heat transfer abilities of cross flow arrangement. One stream flows in a straight flow path along the exchanger and the other stream flow in a zigzag manner at right angles to the direct flow stream thereby covering the entire exchanger in a counter flow manner. This is used mostly when both the streams have varying pressure drops and volume flow rates.

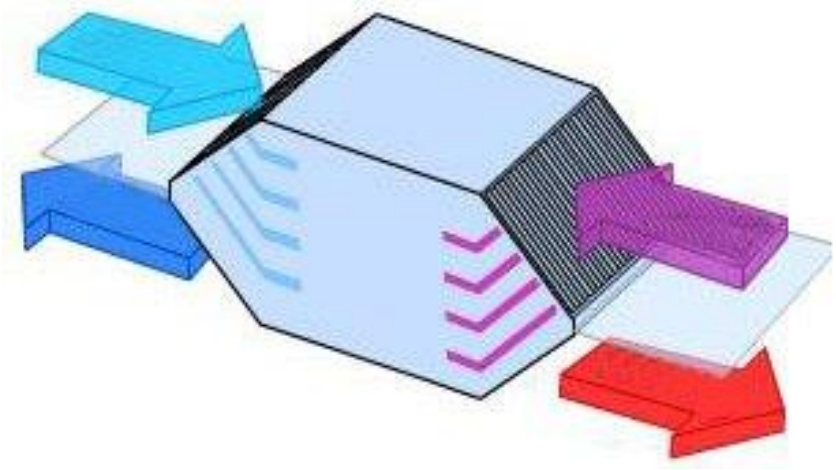

Figure 1.6 Cross-counter flow pattern

1.4.Heat Transfer Surfaces in Plate Fin Heat Exchanger:

The extended surfaces or fins play an important role in the efficiency and effectiveness of the heat exchanger. Due to the low heat transfer coefficient of the gas flow, it becomes obvious that extended surfaces be used to increase the heat transfer rate as mostly the plate fin type heat exchangers are adopted for gas-gas flows. This resulted in the study of a wide variety of plate fins with varied geometries.

The plate fins are classified basically into two types:

1. *Continuous fin type:*

   In this type of fin the extended surfaces form a regular and continuous pattern without any interruption in its form. Due to the sudden variation in the direction of the flow, the temperature gradients formed near the surfaces increase that comes as a bright side. But on the other hand it also results in the increment of the pressure drop and friction factor. Examples of this type are plain fins of rectangular or trapezoidal cross-sections and wavy fins.

2. *Discontinuous fin type :*

   The fin geometry in this type of fin is irregular and interrupted and the flow is also effected greatly due to this. These type of fins have more heat transfer performance than the continuous type as these interrupted passages tend to break up the boundary layers formed resulting in the increment of heat transfer coefficient at the expense of higher pressure drops across the length of the heat exchanger. For a specific dimension of the heat exchanger, the discontinuous type (offset-strip fin) have more frontal area than the continuous type (plain fin). Construction is done either by slitting of the continuous type fins and moving them laterally (*offset strip*) or cutting the fins and bend them down (*louvered fins*) or by punching holes of certain dimensions at regular intervals on the fins (*perforated fins*).

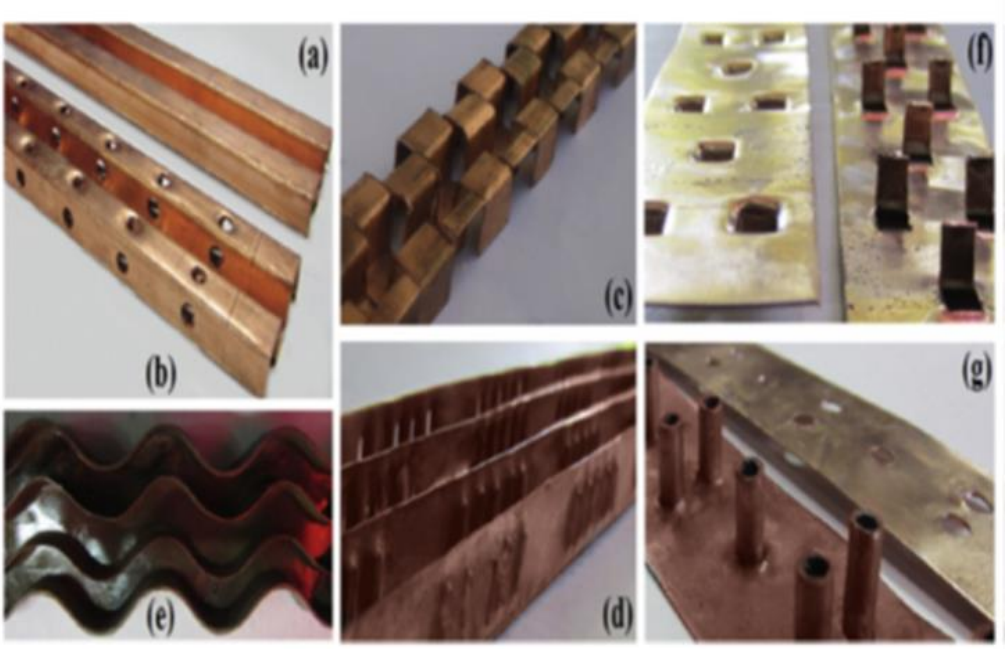

Figure 1.7 Plate-fin channels: (a) plain (b) perforated (c) offset strip (d) louvered (e) wavy (f) vortex-generator (g) pin [1]

On a general basis, the plate fins are classified as:

1. Plain fins
2. Wavy fins
3. Offset-strip fins
4. Louvered fins
5. Perforated fins
6. Pin fins

Close inspection reveals that near the leading edge of the freshly formed boundary layers, the values of heat transfer coefficients and due to which the friction factor values are pretty high.

In general, there are two types of drag occurring near the boundary layer,

a) Friction drag: formed due to the high heat transfer coefficients
b) Form drag: developed due to the definite thickness of the fin.

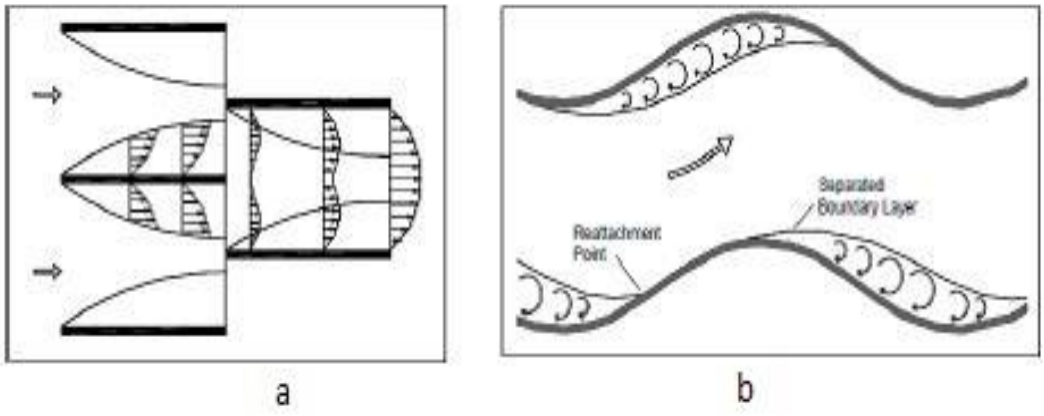

Figure 1.8 Description of boundary layer during flow in a) offset-strip and b) wavy fin [2]

1.5. Colburn Factor, j and Friction Factor, f:

The prediction of the thermal and hydraulic performance factors is the utmost important task in the study of heat exchangers. Non-dimentionalised factors such as the colburn factor j and the friction factor f are used in the evaluation of the heat transfer coefficient and pressure drop characteristics. The design of the heat exchanger also requires the above two factors.

The Colburn factor, j is given as a function of Prandtl number and the Reynolds number. It is crucial in determining the heat transfer coefficient of the fluid flowing. The Colburn factor is given by;

$$j = \frac{h}{GC_p}\mathrm{Pr}^{0.667} \tag{1.1}$$

h =heat transfer coefficient (W/m^2-K)

G= Mass flux ($kg/s\text{-}m^2$)

C_p= specific heat (kJ/kgK)

This factor further is helpful in the various correlations developed by the investigators to evaluate the fluid flow properties.

Mostly the heat exchanger is used in the gas-gas heat transfer where its effectiveness is high. The problem with the gas- gas type of flow is that they require comparatively more pumping power in the distributors than the gas-liquid or liquid-liquid arrangements. Thus it becomes very important to calculate the flow friction characteristics to ensure highest possible efficiency and lowest possible friction. Hence friction factor comes into play to provide with an idea of the level of friction in the heat exchanger's flow passages. The main use of friction factor is in the evaluation of pressure drop. Thus the friction factor is given by;

$$f = \frac{\tau}{0.5\rho v^2} \tag{1.2}$$

f= Fanning friction factor

τ= wall shear stress (N/m^2)

ρ= fluid desity (Kg/m^3)

v= velocity of the fluid (m/sec)

The pressure drop is given by;

$$\Delta p = \frac{4fLG^2}{2D_h\rho} \tag{1.3}$$

h =heat transfer coefficient (W/m^2-K)

G= Mass flux ($kg/s\text{-}m^2$)

L= Length of flow passage (m)

D_h =Hydraulic diameter (m)

ρ=fluid density (mean) (kg/m^3)

The ratio of j/f is known as the Goodness factor of the heat exchanger or to be specific the flow area goodness factor. The need for this factor aroused when the j and f graphical representation did not reveal much information about the relative performance of the different extended surfaces. The main advantage of this factor is that it provides the basic insight into the performance of different extended surfaces before the application of any other design correlation and also can be used for the filtering of these surfaces.

According to Manglik et al [ ], the higher values of j/f denote a lower frontal area for the heat exchanger.

The j and f factors depend on to some extent on the geometrical parameters such as fin length(l), fin height(h), fin spacing(s), fin thickness(t), etc. and this reveals that experimental determination of these factors has to be done especially for cryogenic fields that is considered to be critically designed field. For other applications the numerical analysis of these factors would suffice.

1.6. Objectives:

The important objective of this study is to understand the plate fin heat exchanger working at the cryogenic temperature range (of 80K-110K) using the cold layer test method. The objectives include:

1. To determine performance factors of the heat exchanger like effectiveness and pressure drop at cryogenic temperatures by rating the heat exchanger using different correlations.
2. Using the simulation software Aspen MUSE [3] to simulate the working conditions at cryogenic temperatures at different inlet mass flow rates and derive the effectiveness and pressure drop at each mass flow rate.
3. To compare the results obtained from cold and hot layer tests using Aspen MUSE [3]

1.7. Organisation of the Thesis:

This thesis has been organised into seven chapters taking into account the references.

Chapter 1 discusses the introduction of the plate fin heat exchangers and also the objectives of the present study.

Chapter 2 gives us a concise study and survey of significant literature about the topics under the present investigation and highlights the literature of the various correlations that are to be used in the investigation.

Chapter 3 explains in detail about the experimental set-up and different components used in the investigation.

Chapter 4 gives us an insight into the simulation software by AspenTech for plate fin heat exchangers Aspen MUSE [3].

In chapter 5 the rating, i.e., calculation of the different performance factors like the heat transfer coefficient, effectiveness, friction factor and pressure drop at a specified mass flow rate for the plate fin heat exchanger on which our investigation is based.

Chapter 6 discusses the results obtained by the simulation software Aspen MUSE [3].

And lastly chapter 7 is allotted for the conclusions drawn from the present investigation and the purview of future work.

CHAPTER-2

Literature Review

2. LITERATURE REVIEW

If heat transfer are the principles and heat exchanger is the invention using these principles then the compact heat exchanger is the innovation that has revolutionised the principles of heat transfer.

This literature review discusses briefly about the compact heat exchanger, the plate fin heat exchanger and one of its heat transfer surfaces, i.e. the offset strip fins (OSF) with its heat transfer and flow friction characteristics or in other words the Colburn factor, j and the friction factor, f. also discussed are the various correlations formulated by the respective investigators on these factors. A review about the various anomalies in heat transfer in the plate fin heat exchanger is also presented in this chapter.

Whenever compact heat exchangers are discussed the work of Kays and London [4] is always mentioned first. They were responsible for the in depth study and experimentation of the heat exchangers with various types of the extended heat transfer surfaces. Shah [5] in his book has explained the design process of the compact heat exchangers. Hesselgreaves [6] explained the various types of compact heat exchangers in detail in a more industry application point of view in his book. Cowel et al [7] explained the importance of the compact heat exchangers in the automobile industry.

Kays and London [4] experimented with the plate fin heat exchanger using different heat transfer surfaces on that test heat exchanger to note the dependency of the geometrical factors on the heat transfer and pressure drop characteristics of a plate fin heat exchanger. They used a cross flow type heat exchanger allowing with the surface that is to be experimented with to be the one for the fluid flow using the steady state technique.

The offset strip fins (OSF) are most characterised type of extended heat transfer surface that is experimented with in the plate fin heat exchanger. In an extension to the above work, London and Shah [8] tested eight configurations of the OSF, presenting the heat transfer and related design data for each one of them and it also includes testing of one of the compact heat exchanger of that time of surface density 5885 m^2/m^3. Jacobi et al [9] studied and experimented on the louvered fin on a wind tunnel and presented the related heat transfer and pressure drop relations. They also discussed the effects of the vortex-

shedding phenomenon on the arrays based on the lines of the offset fin arrays. Dong et al [10] conducted experiments on the offset [11] strip fins using 9 heat exchangers with different fin geometries to determine the performance characteristics of the OSF and correlate them with the experimented fin geometry. Ghosh [12] in his PhD thesis work has experimented with the 3 wave and 6 offset strip fin geometry and validated the correlations given by Maiti – Sarangi [22].

Zenner [13] constructed a test rig to test various types of fin configurations. The test exchanger served the purpose of an air cooler for the compressor. The test rig consisted of a wind tunnel using a working fluid as water and at the j-factor at different mass flow rates was evaluated. Dubrovsky [14] experimented on several rectangular and triangular offset strip fins to study the frontal area available and to show the importance of the Nusselt number on the fin geometry. Also the heat transfer and pressure drop singulars were obtained from the experimentation for the various channels. The PhD dissertation of Alur [2] also finds special mention regarding the experimental analysis of plate fin heat exchangers and the friction factor and Colburn factor comparison with the theoretical correlations.

Inspite of the experiments carried out for uncomplicated geometries, other than the hydraulic diameter (D_e), the various fin parameters like fin spacing(s), fin length (l), fin thickness (t), etc. have to be correlated. This is somewhat a difficult and costly affair for the complicated geometries. Hence to save from the agony, we use numerical tools such as CFD to predict and ascertain the thermal parameters for performance.

Patankar et al [11] developed mathematical models and solutions to the fully developed region in the fluid flow for the constant flux or the constant wall temperature conditions. The model takes in the temperature dissemination under any of the conditions as the input and the solution gives the length of variation of the period of the fluid's entrance length to be able to be a fully developed flow. Carrying forward the work, Patankar and Prakash [15], derived experimentally based on the computational results on their previous paper the significance of the plate thickness of the non-continuous type of fins, by taking parameters such as fin thickness ratio t/H and fin length ratio L/H for the range of Reynold number ranging from 100 to 2000. The outcome being that with increasing plate thickness the pressure drop increases. The friction factor were in agreement with that obtained from the equation from Kays and London [4]. Suzuki et al

[16] discussed the problem of the thickness of the fin in the staggered and interrupted array and the repercussion of turbulence occurring at free- stream while taking the numerical based route following the elliptical differencial equations that regulate the progress of momentum and energy. A low Reynolds number range(<800) is considered keeping in mind that a heat exchanger with the offset strip fin has to be constructed for utilising the heat from waste gas. Further it has been shown that the Colburn factor, j yields higher values as compared to that of the experimental values. Also the friction factor, f has found to be in agreement with that of the experimental results.

Zhang et al [17] in their work have computed the solution of the discretised and unsteady Navier-Stokes equation with correlating the thermal parameters for performance measurement like the Colburn factor, j and the friction factor, f at various Reynolds number. It has been found that at low Re no., the j and f factors are in perfect accordance but as the Re no. increases the variation between them also increases resulting in the over forecasting of the j and f factors at Re>1300 and the reason to this is explained to be the three dimensional effects that come into play at high Reynolds number. There are fluctuations in the values of j and f factors in the context to the 2-dimention and 3-dimension flow field simulation.

Shah et al [18] developed CFD modelling on three OSFs' and 16 wavy type fin surface configurations to investigate the flow distribution. These simulations have been validated by the performance of experiment of three types of heat exchanger by varying the flow rate, temperature and pressure drop across the heat exchanger that also includes the drop in pressure at the headers and nozzles. The calculations and experimentation has been done in real and ideal cases. The results obtained for the j and f factors show a variation of ±2% in j factor and ±9 in case of f factor when compared with the singular curves obtained from London and Shah [8].

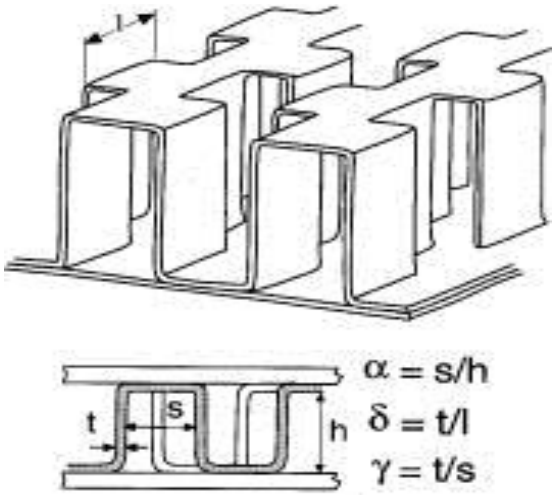

Figure 2.1 OSF geometry [19]

Correlations are required to analytically predict the j and f factors for evaluating the heat transfer coefficient and the pressure drop singulars. Various investigators have given their correlations to fulfil the analytical demand for solution.

An attempt to predict the j and f factors through correlations was made by Manson [20], experimenting with all of the geometries of the heat transfer surfaces. Kays [21] also gave a relationship between the various geometrical parameters and the j and f factors for the OSFs'. The correlation given by Kays [21] is valid for any Reynolds number;

$$j = 0.665\,\mathrm{Re}_l^{-0.5} \tag{2.1}$$

$$f = 0.44(\frac{t}{l}) + 1.328\,\mathrm{Re}_l^{-0.5} \tag{2.2}$$

Tinuat et al [22] formulated a general empirical correlation for the parallel flat plates that are to be utilised by the offset strip fins also. The validation of these correlations was done by experimenting using the above two kinds of fins with water flowing in the rough side if the fins and engine oil flowing in the smooth side of the fin. These correlations have been matched with Weiting's [23] for 22 of the fin patterns that he experimented with and it shows that these correlations are in order though in between the Re no. of 200 to 1000, Weiting [23] returns less values by about 35%. His correlations are;

For Re < 1000;

$$j = 0.483(\frac{1}{D_h})^{-0.162}(\frac{s}{h})^{-0.184}\,\mathrm{Re}^{-0.536} \tag{2.3}$$

$$f = 7.661(\frac{1}{D_h})^{-0.384}(\frac{s}{h})^{-0.092}\,\mathrm{Re}^{-0.712} \tag{2.4}$$

For Re > 2000;

$$j = 0.242(\frac{1}{D_h})^{-0.322}(\frac{t}{D_h})^{-0.089}\,\mathrm{Re}^{-0.368} \tag{2.5}$$

$$f = 1.136(\frac{1}{D_h})^{-0.781}(\frac{t}{D_h})^{-0.534}\,\mathrm{Re}^{-0.198} \tag{2.6}$$

Where, the hydraulic diameter is;

$$D_h = \frac{2sh}{(s+h)} \tag{2.7}$$

Joshi and Webb [24] developed analytical models to correlate the j and f factors related to wake region in the boundary layer separation of the fins. OSF arrays were used to anticipate the wake regions during the transition from laminar to turbulent flows. The equation of Reynolds number for the wake width, i.e., the transition Re no. (Re*), was formulated and then j and f factors correlations for the laminar and turbulent flows was given. The correlations are;

For $\mathrm{Re} \le \mathrm{Re}^*$

$$j_c = 0.53(\mathrm{Re})^{-0.5}(\frac{l}{D_e})^{-0.15}(\frac{s}{h})^{-0.14} \tag{2.8}$$

$$f = 8.12(\mathrm{Re})^{-0.74}(\frac{l}{D_e})^{-0.41}(\frac{s}{h})^{-0.02} \tag{2.9}$$

For Re ≥ Re*+1000

$$j_c = 0.21(\mathrm{Re})^{-0.4}(\frac{l}{D_e})^{-0.24}(\frac{t}{D_h})^{0.02} \tag{2.10}$$

$$f = 1.12(\mathrm{Re})^{-0.36}(\frac{l}{D_e})^{-0.65}(\frac{t}{D_h})^{0.17} \tag{2.11}$$

The transition Reynolds number is given as;

$$\mathrm{Re}* = 257(\frac{l}{s})(\frac{t}{l})D_e(t + 1.328(\frac{\mathrm{Re}}{lD_e})^{0.5})^{-1} \tag{2.12}$$

Free Flow area, A_c = (s-t) h

Heat transfer area, A = 2(sl+ht+hl)

Hence, Hydraulic Diameter is given as;

$$D_h = \frac{2(s-t)h}{(sl+ht+hl)} \tag{2.13}$$

Again, Manglik and Bergles [19] gave their share of empirical correlation by analysing 18 varied exchanger cores to correlate the j and f factors with fin parameters such as s/h, t/l, t/s with the involvement of the Reynolds number. The numerical and experimental data show a discrepancy of ±20% that can be said to hold good for the correlations. They emphasised on the goodness factor j/f being responsible for the frontal area specification in a heat exchanger. These correlations are specified to provide information about both the laminar and turbulent flows,

$$\begin{aligned} j = {} & 0.6522\,\mathrm{Re}^{-0.5403}(\frac{s}{h})^{-0.1541}(\frac{t}{l})^{0.1499}(\frac{t}{s})^{-0.0678} \times \\ & [1 + 5.269\times10^{-5}\,\mathrm{Re}^{1.340}(\frac{s}{h})^{0.504}(\frac{t}{l})^{0.546}(\frac{t}{s})^{-1.055}]^{0.1} \end{aligned} \tag{2.14}$$

$$f = 9.6243\,\mathrm{Re}^{-0.7422}\left(\frac{s}{h}\right)^{-0.1856}\left(\frac{t}{l}\right)^{0.3053}\left(\frac{t}{s}\right)^{-0.2659}\times$$
$$\left[1+7.669\times10^{-8}\,\mathrm{Re}^{4.429}\left(\frac{s}{h}\right)^{0.920}\left(\frac{t}{l}\right)^{3.767}\left(\frac{t}{s}\right)^{0.236}\right]^{0.1} \quad (2.15)$$

Here, the Free Flow Area, $A_c = sh$

The Heat transfer area, $A = 2(sl+ht+hl) + ts$

So the Hydraulic Diameter is given as;

$$D_h = \frac{4shl}{2\left(sl+ht+hl\right) + ts} \quad (2.16)$$

Maiti and Sarangi [25], in their PhD dissertation used CFD modelling to devise the correlations to associate the j and f factors with geometrical actors if the fins. Also the concept of multiple regression analysis was utilised to help the finding of constants to be used in the correlations. Some of the constants were also extracted by experimental compilations. The transition state Reynolds number also finds importance in these correlations and which has been devised separately for the heat transfer coefficient and pressure drop singulars. The correlations are stated as below;

For laminar range, $\mathrm{Re}\leq\mathrm{Re}^*$

$$j = 0.36(\mathrm{Re})^{-0.51}\left(\frac{h}{s}\right)^{0.275}\left(\frac{l}{s}\right)^{-0.27}\left(\frac{t}{s}\right)^{-0.063} \quad (2.17)$$

$$f = 4.67(\mathrm{Re})^{-0.7}\left(\frac{h}{s}\right)^{0.196}\left(\frac{l}{s}\right)^{-0.181}\left(\frac{t}{s}\right)^{-0.104} \quad (2.18)$$

For turbulent range, $\mathrm{Re}>\mathrm{Re}^*$

$$j = 0.18(\mathrm{Re})^{-0.42}\left(\frac{h}{s}\right)^{0.288}\left(\frac{l}{s}\right)^{-0.184}\left(\frac{t}{s}\right)^{-0.05} \quad (2.19)$$

$$f = 0.32(\mathrm{Re})^{-0.286}(\frac{h}{s})^{0.221}(\frac{l}{s})^{-0.185}(\frac{t}{s})^{-0.023} \quad (2.20)$$

The transition Reynolds no. for the heat transfer coofficient is given as;

$$\mathrm{Re}* = 1568.58(\frac{h}{s})^{-0.217}(\frac{l}{s})^{-1.433}(\frac{t}{s})^{-0.217} \quad (2.21)$$

The transition Reynolds no. for the pressure drop singulars is given as;

$$\mathrm{Re}* = 648.23(\frac{h}{s})^{-0.06}(\frac{l}{s})^{0.1}(\frac{t}{s})^{-0.196} \quad (2.22)$$

Free Flow area, $A_{c=}$ (s-t) h

Heat transfer area, A = 2(sl+ht+hl)

Hence, Hydraulic Diameter is given as;

$$D_h = \frac{2(s-t)h}{(sl+ht+hl)} \quad (2.23)$$

Plate fin heat exchangers are a lucrative equipment in the field of cryogenics and aerospace applications owing to their significance, but their performance degrades due a lot of factors that tend to undermine the full extent utilization of the heat exchanger. The factors can be the heat transfer losses occurring to the outside system, or the axial or longitudinal conduction of heat along the walls of the fluid streams or the misdistribution of flow.

In the issue of axial conduction of heat, Barron [26] in his book has discussed this problem undergoing in the heat exchangers that accompanies dual stream of fluid flow. The extent of this factor is measured by the term ineffectiveness coined by the pioneer in plate fin heat exchanger study, Kays and London [4]. The ineffectiveness is correlated by the factor of longitudinal conduction parameter (λ) and is stated as;

$$\lambda = \frac{k_f A_c}{LC_{\min}} = \frac{\delta\varepsilon}{\varepsilon} \quad (2.24)$$

Another extensive work performed on this factor is by Kroeger [27], who gave solutions to the equations regarding the axial conduction of heat in the heat exchangers that accompanies dual stream of fluid flow with OSF arrays. The correlations were given for the balanced and unbalanced flow, C*=1 and C*<1 respectively of fluid streams with including the number of transfer units (NTU) of the heat exchanger into account where the factor (1- ε) is adjudged as the ineffectiveness of the system.

Another important team of investigators regarding the research in the longitudinal conduction of heat in plate fin heat exchangers is the team of Venkatarathnam and Narayanam [28] , who also studied the longitudinal conduction of heat from the walls of the heat exchanger apart from that of due to the walls between the fluid streams. They too gave their correlation based on the NTU, λ and ineffectiveness.

The above calculation of ineffectiveness are based on the high temperature regions and for the plate fin heat exchanger to be used in the cryogenic fields, the longitudinal heat conduction must be understood at those temperature levels. A step in this area has been taken by Gupta and Atrey [29] who did their research work on the heat ins leak and flow misdistribution at the temperature ranges of 300 to 80K and 80-20K. They did refer to their previous work (Gupta et al [30]) for the numerical model for longitudinal heat conductuion of tube-in tube heat exchanger but in this paper they did also consider the heat in leak parameter also. A term degradation factor τ was also coined to determine the effects of heat leak from the atmosphere also the axial conduction from the wall. Degradation factor τ is expressed as;

$$\tau = \frac{\delta\varepsilon}{\varepsilon} \tag{2.25}$$

CHAPTER-3

Experimental Set-Up and Procedure:

3. EXPERIMENTAL SET-UP AND PROCEDURE:

This chapter deals with the experimental set-up and its components up on which the simulation is carried. The various P&I diagram, the manufacturer's design of the plate fin heat exchanger is shown along with the actual photographs.

Also explained is the procedure to be followed for the experimentation and the method of testing of the heat exchanger.

3.1. Equipments:

3.1.1. Plate Fin Heat Exchanger:

The plate fin heat exchanger is an all aluminium heat exchanger made of aluminium alloy Al-3003 to be used in the simulation is a counter flow offset strip fin surface characterization. It was manufactured by Mesons Apollo Heat Exchangers, Mumbai for the Bhabha Atomic Research Centre (BARC) and was deployed to NIT Rourkela for the purpose of the analysis of performance factors and to correlate the j and f factors. The diagram with the manufacturing point of view has been shown in Fig.3.1 with all of its components and their respective dimensioning. The high pressure side has 5 layers and the low pressure side has 4 layers and the testing method must be in relation with this data. Further data has been provided with in table 3.1. Also the core dimensions and fin geometry data has been tabulated in tables 3.2 and 3.3 respectively. The design data for tis heat exchanger is given in table 3.4 and this basically built to operate at high pressures and low temperatures.

Table 3-1 Flow arrangement of the heat exchanger

	HIGH PRESSURE SIDE (Hot Fluid Side)	**LOW PRESSURE SIDE (Cold Fluid Side)**
FIN	Offset-Strip Fin(OSF)	Offset-Strip Fin(OSF
NO. OF PASSAGE	5	4
NO. OF PASS	1	1
FLOW PATTERN	COUNTER FLOW	COUNTER FLOW

Table 3-2 Core dimensions of heat exchanger

CORE LENGTH	900 mm
CORE WIDTH	73 mm
CORE HEIGHT	93 mm
TOTAL LENGTH	1000 mm
TOTAL WIDTH	85 mm
TOTAL HEIGHT	105 mm

Table 3-3 Fin geometry of heat exchanger

	FIN GEOMETRY	**HIGH PRESSURE SIDE(Hot Fluid Side)**	**LOW PRESSURE SIDE (Cold Fluid Side)**
1	Fin frequency, f	714 fins /metre	588 fins/ metre
2	Fin length, l	3 mm	5 mm
3	Fin thickness, t	0.2 mm	0.2 mm
4	Fin height, h	9.3 mm	9.3 mm
5	No. of layers	5	4

Table 3-4 Design data of the heat exchanger

	HOT SIDE	**COLD SIDE**
FLUID	HELIUM(HP)	HELIUM(LP)
FLOW RATE	5 g/s	4.8 g/s
INLET TEMPERATURE	310K	83.65 K
OUTLET TEMPERATURE	92.85 K	301.67 K
ALLOWABLE PRESSURE DROP	0.05 bar	0.05 bar
PRESSURE AT INLET	7.35 bar	1.15 bar
HEAT LOAD	5.5 KW	5.5 KW

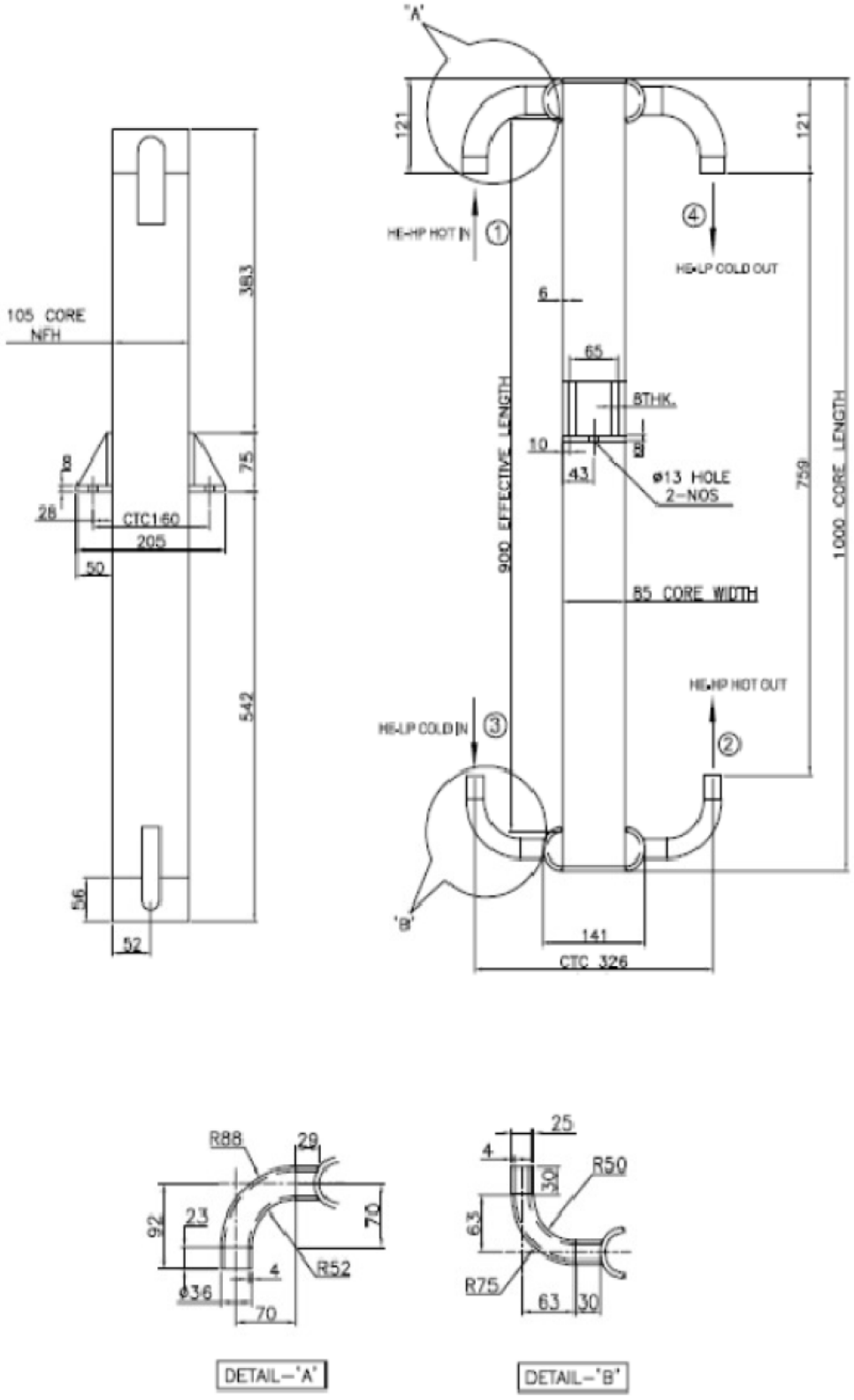

Figure 3.1 Details of the test heat exchanger

3.1.2. Compressor:

A positive displacement type twin screw rotor compressor manufactured by KAESER KOMPRESSOREN GmBh has been used as inlet supply for the test heat exchanger. It has two similar size rotors, one called the male rotor and the other the female rotor. The female rotor has more lobes than that of the male one. The gas passes through these lobes and simultaneously gets compressed along the length. The rotors are in constant rotation and in constant mesh with each other to allow the compression to occur. Their relatively high rotational speeds is the reason that makes them much compact than their other types of positive displacement compressors. The need for high operating pressures and volume rates has made the industrial fields and other professional fields to adopt this type compressor as their working compressor for almost all applications.

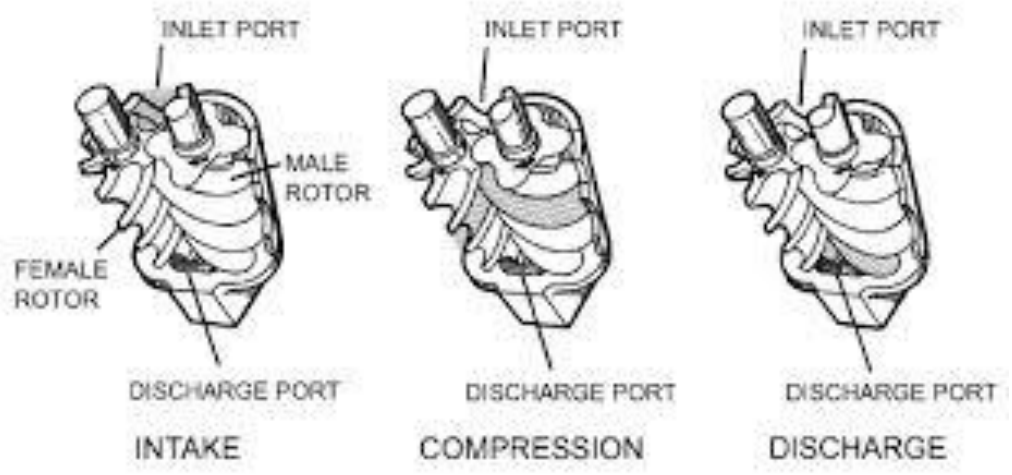

Figure 3.2 Twin screw compressor

The Compressor specification is given below:

Table 3-5 Compressor specifications

Make	Kaeser Kompressoren GmBh
Model	BSD 72
Profile of Screw	Sigma
Free air delivery	336 m3/hr
Suction Pressure	Atmospheric
Maximum Pressure	11 bar
Operating temperature	75-110°C
Motor	37kW, 74 amps, 3Φ, 50Hz, 415V±10%, 3000rpm

3.1.3. Chiller:

The chiller unit consists of coil type heat exchanger inside an insulating vessel. Cooling chamber (chiller) is used to supply cold gas to the plate fin heat exchanger where the insulating vessel shall contain liquid Nitrogen (at 77K). It is designed and developed in our cryogenics lab. It is basically having a shell and tube type of heat exchanger having a coil length of 7m.

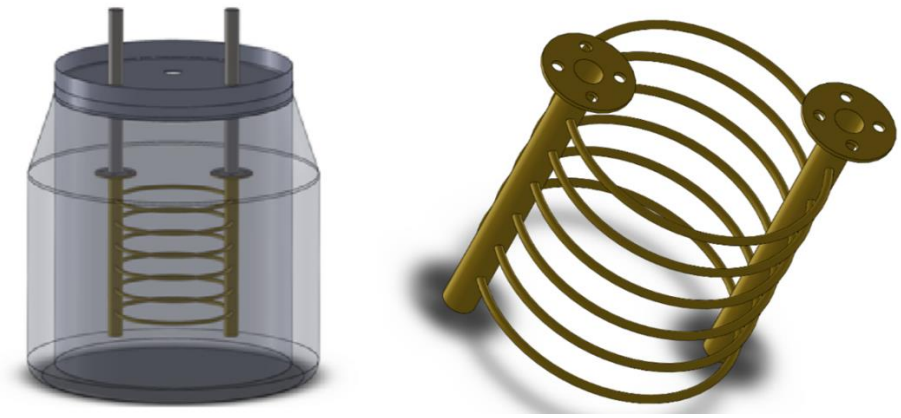

Figure 3.3 Chiller unit and the shell and tube heat exchanger

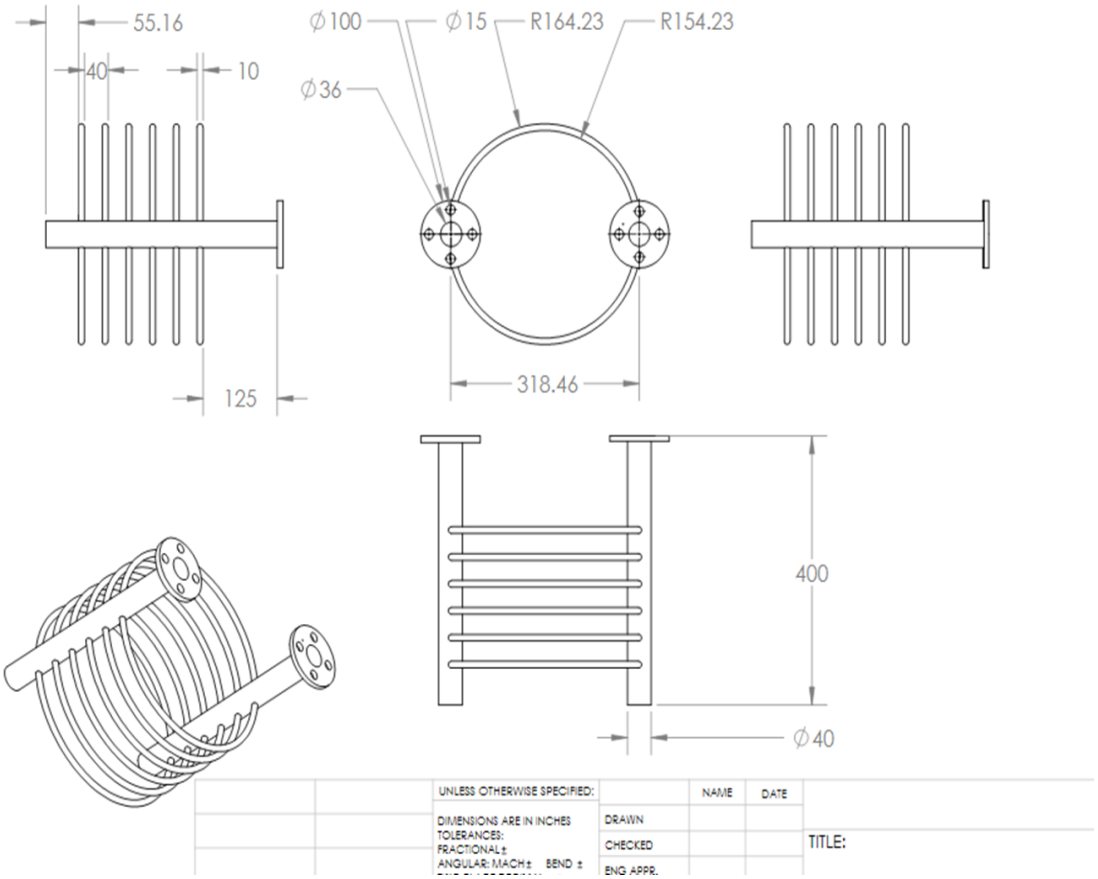

Figure 3.4 Details of the shell and tube heat exchanger in the chiller

3.1.4. Resistance temperature detectors (RTD):

The concept that the electrical resistance of metals increases with temperature is utilised in resistance thermometers. These are used mainly for the accurate measurements of below 150°C.

An elementary RTD utilises a resistance offering component, electrical load and an instrument for gauging resistance. The resistance offering component is sensitive to temperature changes of which concept is being used in the RTD. This component is enclosed in a protecting tube and arrangement is made for the electrical contacts to be used readily. The component that is used to provide resistance should not change its properties, physically or chemically, with the respective variation in temperature. This is to ensure that at any temperature, the resistance of the component can be reproduced. Fitting the requirements stated above is the metal Platinum (Pt) and the RTD made from this metal can measure temperatures up to accuracy of ±0.01°C while offering its service quite

efficiently at low temperatures also. The fragile thin wire offering resistance that is in a coiled form is encapsulated in a tube of quartz.

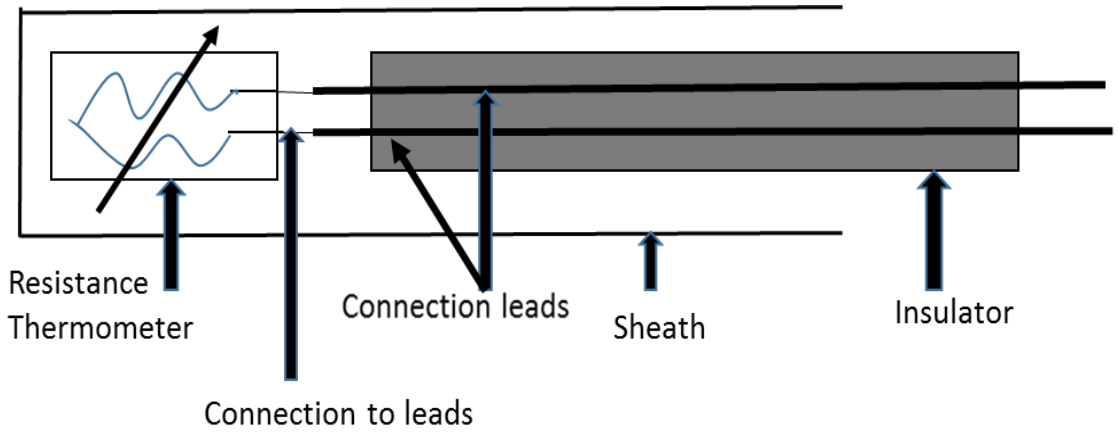

Figure 3.5 Construction of a RTD

There are three types of configuration of the RTD and the choice of the specific configuration depends on the efficiency and the type of measurement instruments.

(a) Two wire composition

(b) Three wire composition and

(c) Four wire composition.

The nominal resistance also called rated resistance is generally taken as the scale of comparison for RTD at a temperature of 0^0C. Pt-100 type of RTD has 100Ω at 0^0C and is the most commonly used. Resistance and temperature follows a very near linear relationship given by;

For < 0^0C $$R_T = R_0[1 + aT + bT^2 + cT^3(T - 100)] \quad (3.1)$$

For > 0^0C $$R_T = R_0[1 + aT + bT^2] \quad (3.2)$$

Where,

R_T = resistance at temperature T

R_0 = resistance at standard temperature

a, b, and c are constants.

3.1.5. Air Dryer Unit:

In a compressed air system, the presence of moisture greatly impacts the efficient and fruitful running of the system. Due to moisture there accumulates dust and scale deposits in the pipes thus increasing the fouling factor that can deviate the experimental results. It is also responsible for increase in the fluid flow resistance and erratic behaviour in the operation of valves, etc. moisture can be removed by two methods:

1. Refrigeration: by decreasing the temperature of the moisture air at a constant temperature results in the saturation of moisture and hence riddance from air.
2. Adsorption: by using desiccants or moisture adsorbing materials. Examples are: silica gel, activated charcoal and alumina, and zeolites.

In this investigation a heatless adsorption dryer manufactured by Delair of model name DC-128 of 291 Nm3/hr (Normal cubic meter) capacity is used. Its use is justified because during the cleaning and maintenance of the piping and valves leading to the test heat exchanger, water and scaling deposits were found.

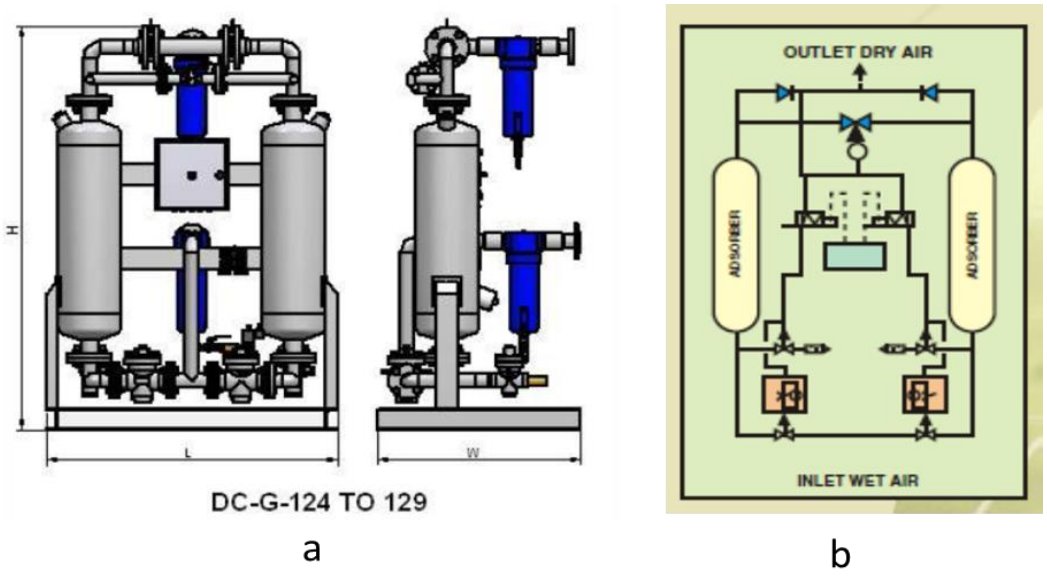

Figure 3.6 a) dimensions of air dryer b) Flow diagram

Table 3-6 Specification of the air dryer

CAPACITY	DIMENSIONS(mm)			WEIGHT
291 Nm3/hr	L	W	H	220 Kg
	1000	700	1450	

3.2 Experimental Test Rig:

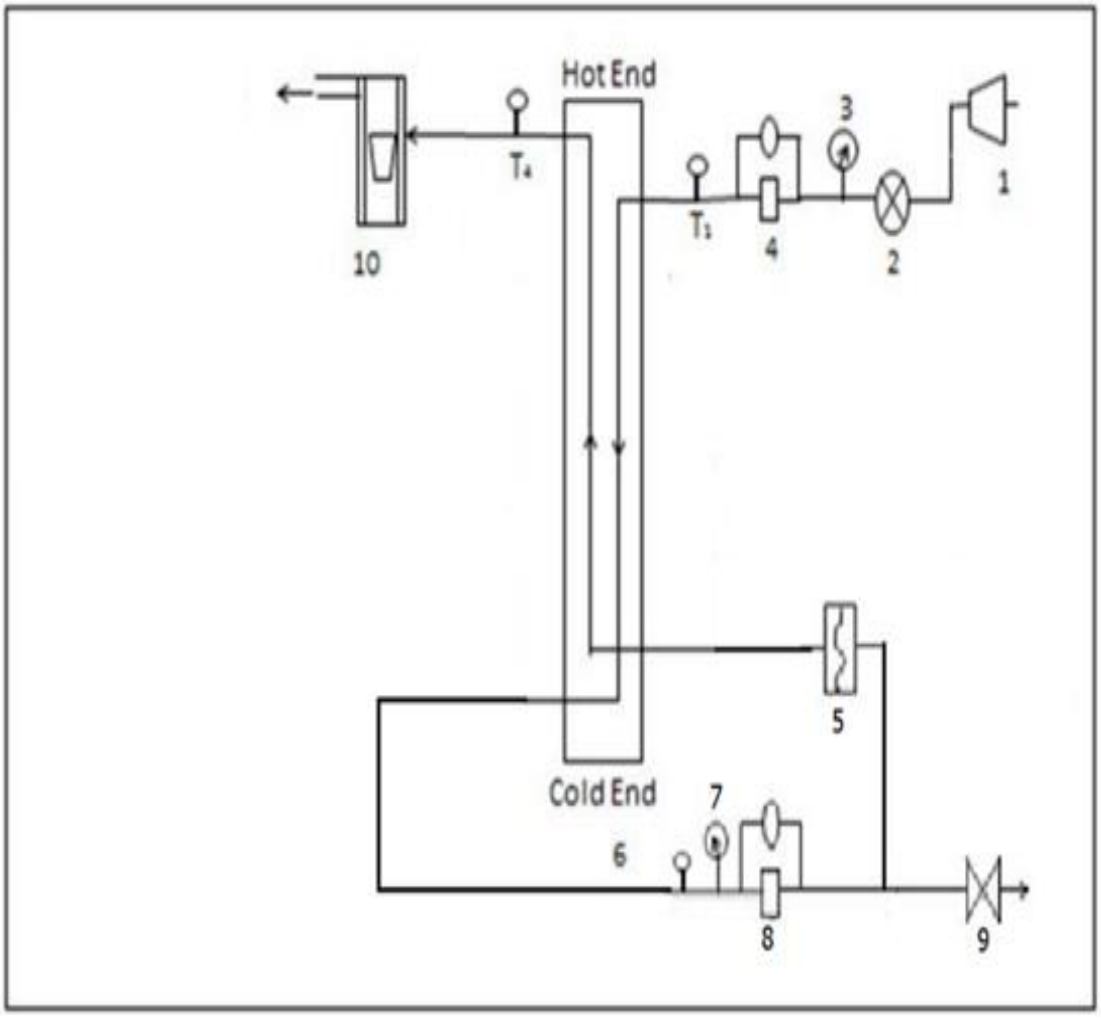

Figure 3.7 P&I diagram of the experimental test rig

1. Compressor	2. Control Valve	3,7 .Pressure Taps
4,8.U-Tube Manometer	5. Chiller	6.Test section
T1,T2,T3,T4-RTDs'	9. Bypass valve	10.Flow meter

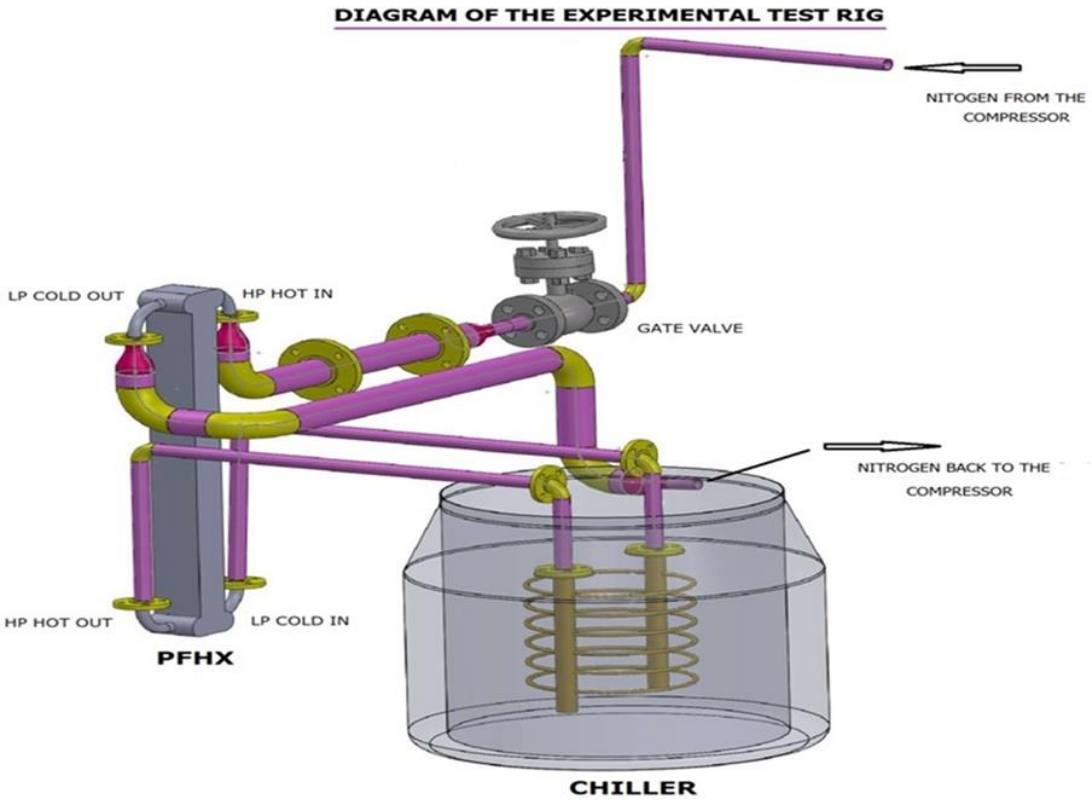

Figure 3.8 Diagram of the test rig

Figure 3.9 Remaining components of the test rig

3.3 Procedure for cold layer test method:

3.3.1. Cold layer test and Hot layer test Method:

Cold layer testing is said to be done when the cold temperature fluid layers are sandwiched between two hot temperature layers. Here the characteristic length for the fin efficiency calculations has to be taken separately for the inner layers and for the outer layers of the fin that is accommodating the hot fluid as the outer layers of the hot fluid are exposed to atmosphere more so the fin efficiency for the inner and outer layer of the hot fluid will vary. Hence there shall be separate fin efficiencies for the inner and outer layers of the fin. On the other hand the characteristic length for the fin accommodating the cold fluid is taken for the inner and outer layers is the same and hence fin efficiency shall also be same.

Hot layer testing is said to be done when the hot temperature fluid layers flows in between two hot temperature layers. Here the characteristic length for the fin efficiency calculations for the inner layers and for the outer layers of the fin accommodating the cold fluid has to be taken as the outer layers of the cold fluid are exposed to atmosphere more so the fin efficiency for the inner and outer layer of the cold fluid will vary. The hot fluid being trapped in between the cold fluid has the same characteristic length for the inner layers and for the outer layers of the fin.

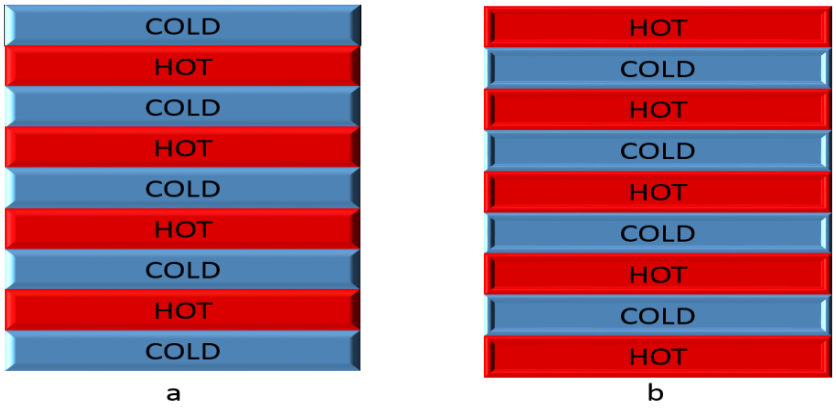

Figure 3.10 Layer wise Diagram a) Hot layer test b) Cold layer test

The simulation of the experimental test rig is done by the cold layer test method in which the cold fluid is sandwiched between the hot layers. Here air used as the working fluid. The air from the compressor first flows to the receiver tank or the buffer tank after which it heads for the Air Dryer unit that then connects to the test heat exchanger through

control valve that is used to control the flow rate of the incoming air. It then enters the chiller unit where the air is cooled to liquid Nitrogen temperatures and also the pressure reduced. The cold air then again enters the heat exchanger enabling the heat transfer between the two fluids.

There are pressure gauges at the inlet and exit to the heat exchanger and the chiller unit for pressure monitoring and also a U-tube manometer is placed near inlet taps of the heat exchanger. The temperatures regarding the entering and exit air is measured by the RTDs'. The rotameter is used to measure the air flow rate of the incoming and exiting air.

CHAPTER-4

Aspen MUSE

4. ASPEN MUSE

This chapter gives a brief introduction about the simulation software MUSE and the figures that follow shall explain the start-up, data input and the output obtained using this software for the simulation of the test heat exchanger that has been explained in the previous chapter.

4.1 Introduction:

In the year 1981, Massachusetts Institute of Technology (MIT) and US Department of Energy led the development of a research project named- *Advanced System for Process Engineering* (ASPEN) that tuned into a full-fledged software solutions enterprise for the process industries.

MUSE [3] is one of the products of AspenTech used for the design and performance simulation of plate fin heat exchangers (PFHE) for two stream or multi-stream fluid flow. It can perform the following calculation modes:

1. *Simulation:*

   On the basis of the entered inlet conditions it gives output regarding the outlet temperatures, the heat loads, pressure drops and the thermos-hydraulic properties along the length of the heat exchanger.

2. *Design:*

   This mode gives a first-hand insight into design of the heat exchanger under a given set of specified heat duty cycles and pressure drop limits which is very useful in a more manufacture's point of view.

3. *Thermosyphon:*

   Thermosyphon is a phenomenon that occurs due to natural convection that helps to circulate the fluid inside a system without the need of a pump.an example of this is the working of a solar heater.

   In this calculation mode, the software gives the performance of the stream that is under the effect of thermosyphon. Input values can be the head of the liquid or the stream flow rate.

4. *Layer by layer simulation:*

   This mode is similar in working to the normal simulation but in this a layer by layer performance is calculated instead of taking the whole stream. The layer pattern can also be specified.

5. *Cross flow heat exchanger:*

   This includes number of passes in a cross flow exchanger and also includes thermosyphon.

MUSE gathers information about the overall geometry, the distributor and nozzle geometry and placement and the type of fin surfaces like plain, wavy, offset strip, etc. of the plate fin heat exchanger. It is basically made of four different calculation engines. They are;

1. *MUSE*: For the thermal performance and simulation of PFHE
2. *MULE*: This is also for the thermal performance and simulation of PFHE but more inclined for the layer simulation.
3. *MUSC*: For the simulation of cross flow plate fin heat exchangers and reboilers.
4. *PFIN*: For the first time design approximations.

4.2 Procedure for the simulation in MUSE:

4.2.1 Start-up:

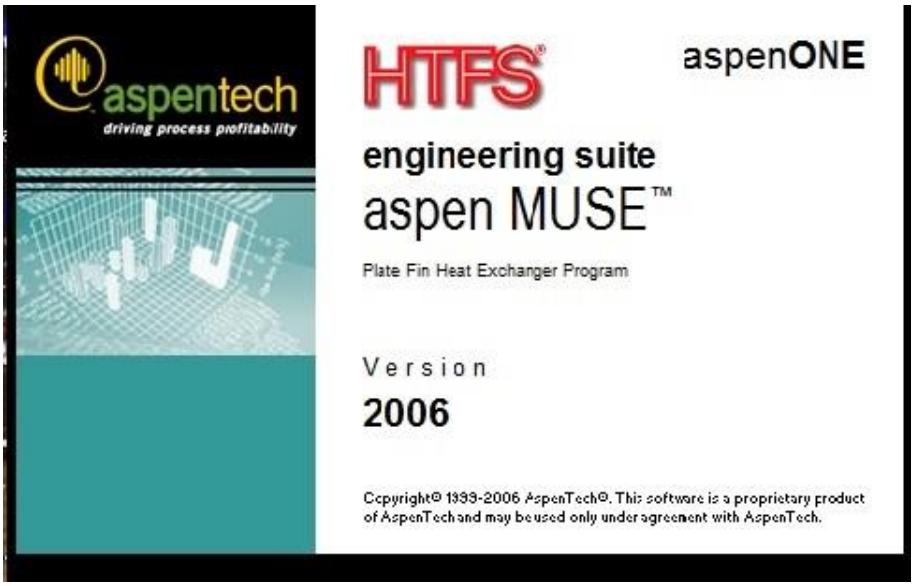

Figure 4.1 Opening of MUSE

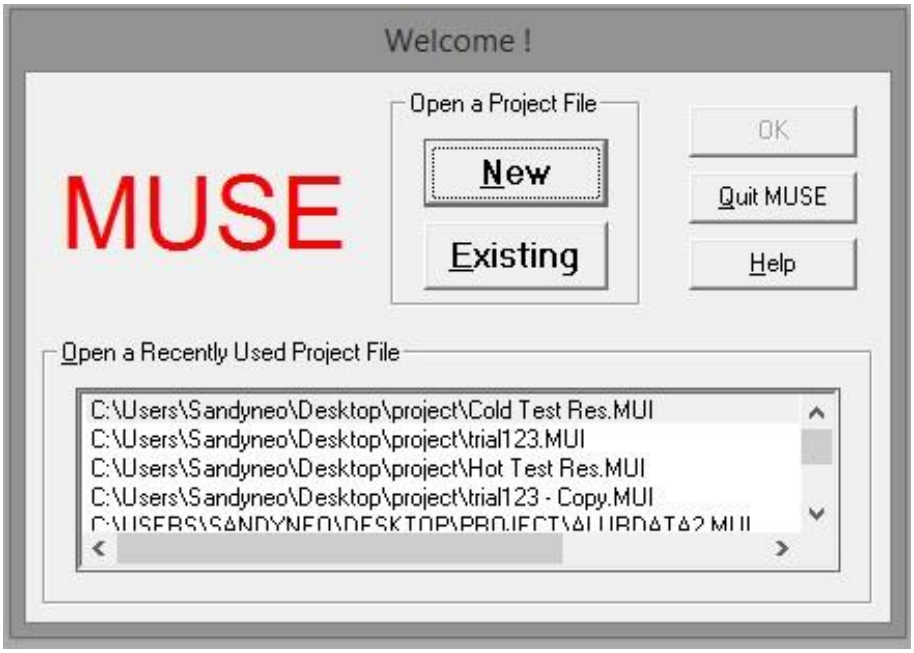

Figure 4.2 File select dialog box

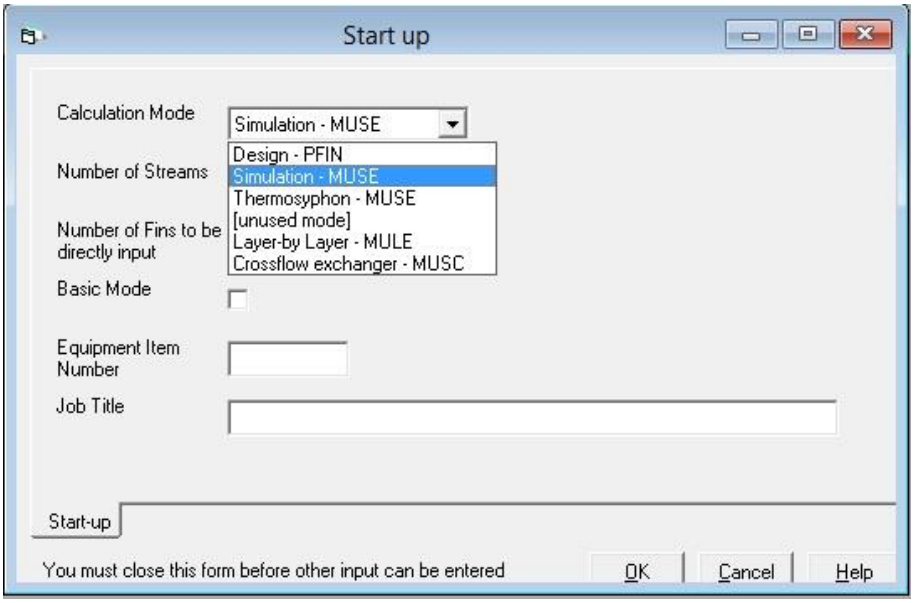

Figure 4.3 start-up menu

The start-up menu is for the selecting of the calculation mode and the details of number of streams and the project title.

4.2.2 Data Input:

1. The first data input is for the geometry of the plate fin heat exchanger where the parting sheet, side bar, cap sheet and the width dimensions. Also the layer pattern, stream geometry and the distributor and nozzle geometry is also entered as shown in Fig 4.4.
2. Next as shown in Fig 4.5 is the process data for the streams where in the values of required mass flow rate, inlet temperature and pressure along with other parameters like estimated pressure drop and fouling resistance are given.
3. The details of fin geometry is entered in the next tab with giving details of fin width, thickness, height and type of fin configuration is given, as Fig 4.6 shows. The details should be in accordance with the actual heat exchanger on which simulation is carried out.

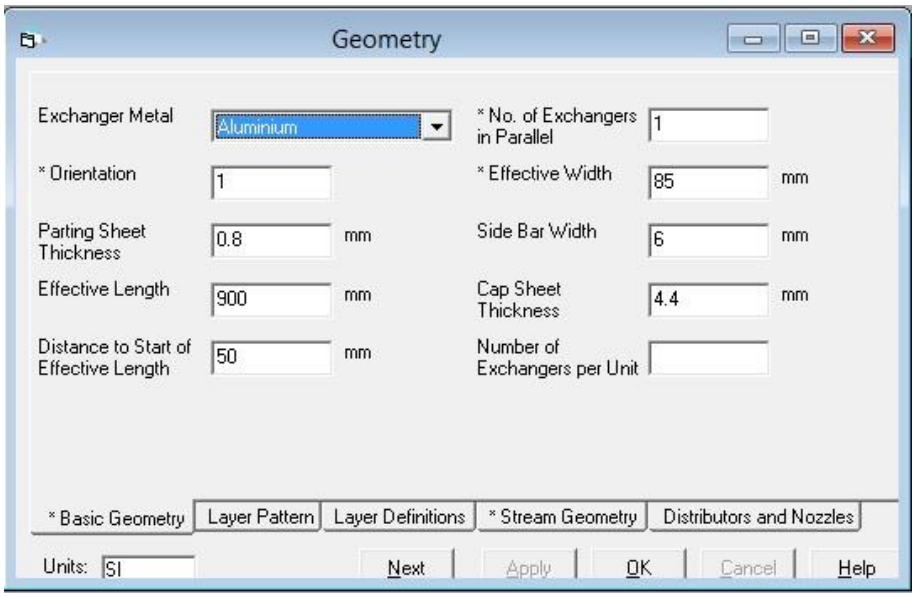

Figure 4.4 Geometry input

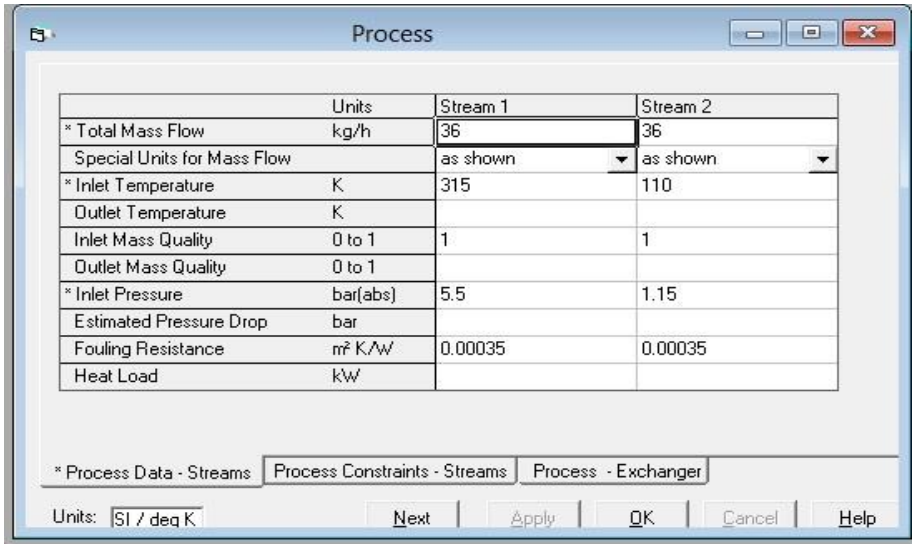

Figure 4.5 Process data input

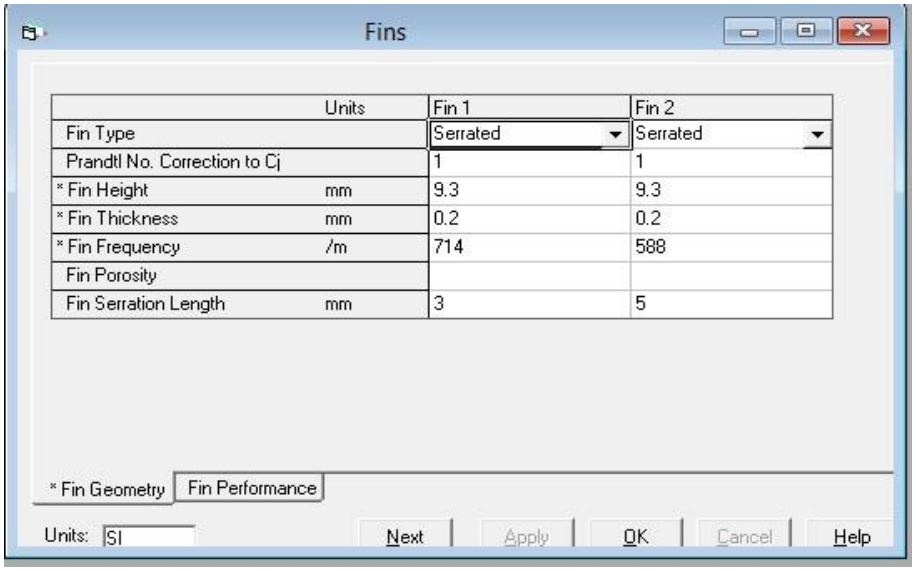

Figure 4.6 Fin geometry input

4. Here for an instance, a set of the inputs is being taken and consequently output is achieved. The data is as follows:

$\dot{m}$ = 36 kg/hr	Thi = 315K	Tci= 110K	ΔPh= 5.5 bar	ΔPc= 1.15 bar	F=0.000035 Km^2/W

5. The longitudinal conduction setting is activated and put to Basic + Fins mode to cover the entire heat exchanger.

4.2.3 Output:

After compiling the input data, it is made to run with the display of errors and warnings (if any), we can see the results in a summary or in a full detailed manner. The respective figures, Fig 4.7, 4.8 and 4.9 are as shown.

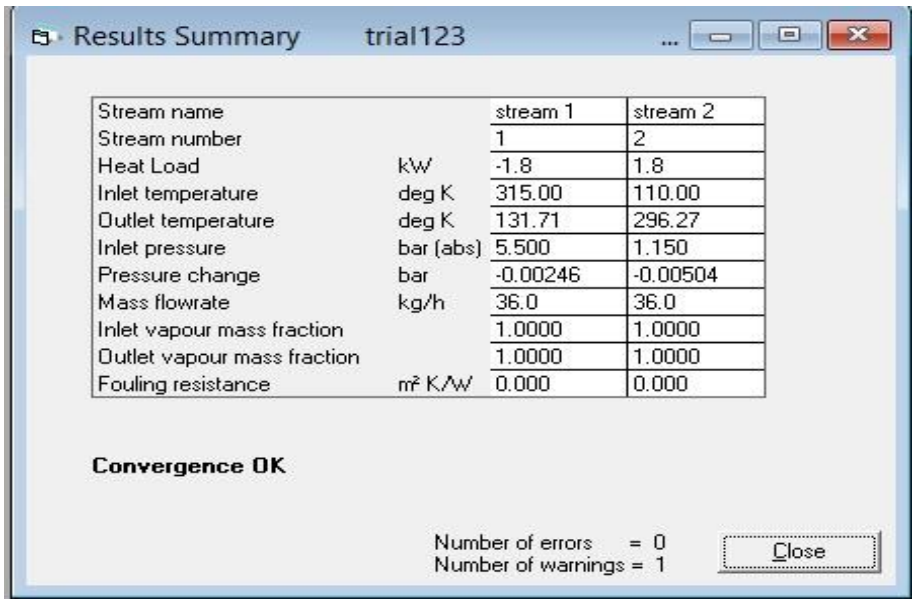

Figure 4.7 Results summary

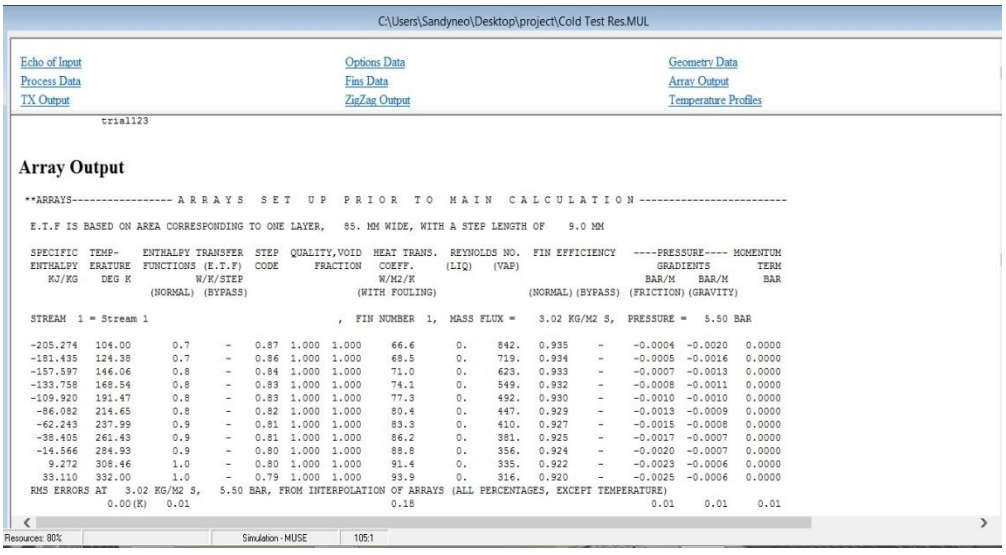

Figure 4.8 Detailed full results-1

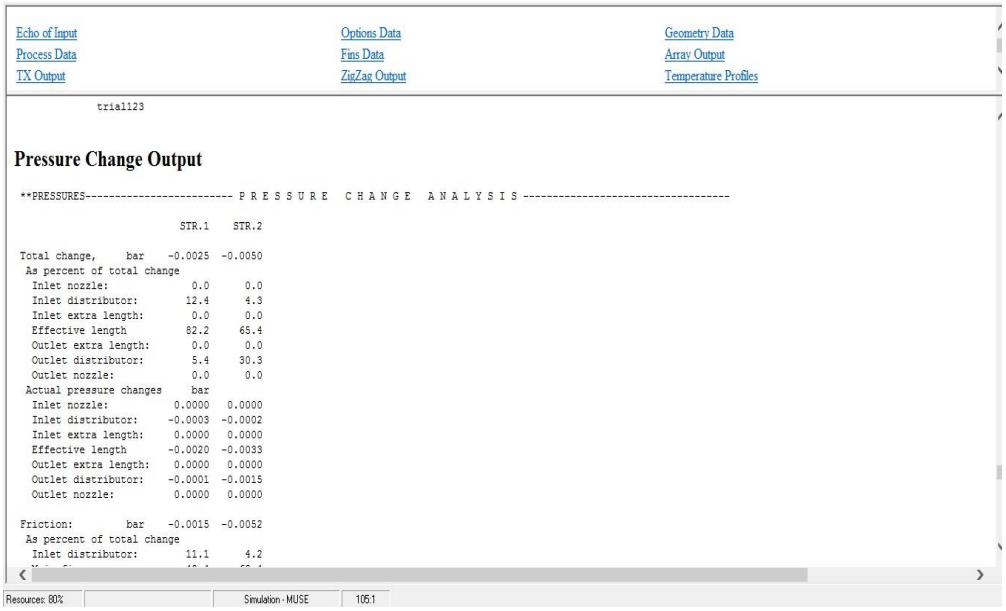

Echo of Input | Options Data | Geometry Data
Process Data | Fins Data | Array Output
TX Output | ZigZag Output | Temperature Profiles

trial123

Pressure Change Output

**PRESSURES---------- P R E S S U R E C H A N G E A N A L Y S I S ----------

		STR.1	STR.2
Total change,	bar	-0.0025	-0.0050
As percent of total change			
Inlet nozzle:		0.0	0.0
Inlet distributor:		12.4	4.3
Inlet extra length:		0.0	0.0
Effective length		82.2	65.4
Outlet extra length:		0.0	0.0
Outlet distributor:		5.4	30.3
Outlet nozzle:		0.0	0.0
Actual pressure changes	bar		
Inlet nozzle:		0.0000	0.0000
Inlet distributor:		-0.0003	-0.0002
Inlet extra length:		0.0000	0.0000
Effective length		-0.0020	-0.0033
Outlet extra length:		0.0000	0.0000
Outlet distributor:		-0.0001	-0.0015
Outlet nozzle:		0.0000	0.0000
Friction:	bar	-0.0015	-0.0052
As percent of total change			
Inlet distributor:		11.1	4.2

Resources: 80% | Simulation - MUSE | 105:1

Figure 4.9 Detailed full results-2

CHAPTER-5

Rating Of Test Heat Exchanger at Cryogenic Temperatures

5. RATING OF TEST HEAT EXCHANGER AT CRYOGENIC TEMPERATURES

Rating of an existing or an already designed heat exchanger involves the finding out of thermal performance factors of a heat exchanger. It is used to find out the heat transfer coefficient, NTU, the friction factor, the pressure drop, etc. of the heat exchanger. The Colburn factor j, and the friction factor f are also found out using the various correlations given.

As the outlet temperatures and the value of effectiveness of the hot and cold fluids are unknown, so we assume a certain value of effectiveness (generally it is taken in-between 75% to 85% for the single pass counter flow heat exchangers) and then calculate the outlet temperatures based on this effectiveness and later the mean fluid temperatures at which we have to determine the fluid properties for the evaluation of the performance factors. The effectiveness when obtained by the correlations is then again used to find out the outlet temperatures. This procedure then becomes iterative until the assumed temperatures and calculated temperatures are similar.

5.1 Steps for Rating:

Here calculation is shown for the hot side fluid and in a similar manner cold side fluid parameters can be calculated. Also Joshi and Webb correlation has been used first and performance factors using other correlations can be calculated in the same way. The various steps used for the rating procedure are as follows:

A. Surface geometrical factors:

   The various dimensions regarding the fin are found out and the values of free flow area, frontal area, hydraulic diameter, etc. are calculated.

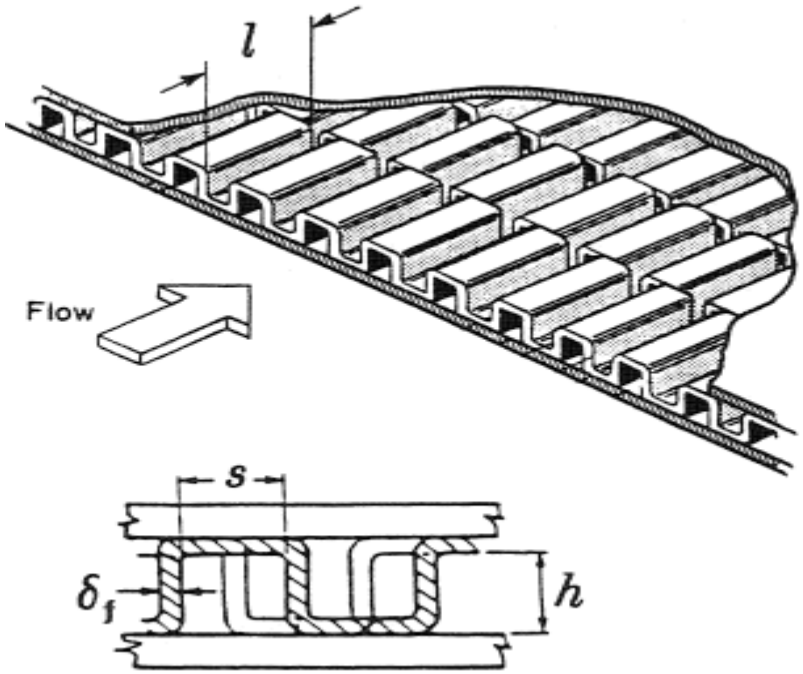

Figure 5.1 OSF Geometry [24]

Table 5-1 Fin Surface Dimensions

	Hot Side	**Cold Side**
Fin height(***h***)	9.3 mm	9.3mm
Fin spacing(***s***)	1.2 mm	1.501mm
Fin thickness(***t***)	0.2 mm	0.2 mm
Fin strip length(***l***)	3 mm	5 mm
No. of layers($\mathbf{N_l}$)	5	4
No. of fins/m ($\mathbf{N_f}$)	714	588
Plate thickness(**a**)	0.8 mm	0.8 mm

a) Fin spacing, $s = \dfrac{1-(N_f \times t)}{N_f} = \dfrac{1-(714\times 0.0002)}{714} = 0.0012$ m

b) Free flow area, $A_{ff} = (s-t)h = (0.0012-0.0002)0.0093 = 0.0000093$ m^2

Frontal area, $A_{fr} = (h+t)(s+t) = (0.0093+0.0002)(0.0012+0.0002) = 0.0000133$ m^2

c) $\sigma = \dfrac{A_{ff}}{A_{fr}} = 0.6992$

d) Heat transfer area/fin, $a_s = 2(ht + hl + sl) =$

$= 2(0.0093\times 0.0002 + 0.0093\times 0.003 + 0.0012\times 0.003) = 0.00006672$ m^2

e) Ratio of area of fin to the heat transfer area,

$$\frac{a_f}{a_s} = \frac{2h(l+t)}{a_s} = \frac{2\times 0.0093(0.003+0.0002)}{0.00006672} = 0.8920$$

f) Equivalent Diameter,

$$D_e = \frac{4\times a_{ff}\times l}{a_s} = \frac{(s-t)h}{2(ht+hl+sl)} = \frac{(0.0012-0.0002)0.0093}{2(0.0093\times 0.0002 + 0.0093\times 0.003 + 0.0012\times 0.003)}$$

$= 0.001673$ mm

g) Distance between plates, b=(h+t)=(0.0093+0.0002)=0.0095 m

B. Heat transfer area, A:

a) Total area between the plates, $A_{fr} = b\times N_l \times W = 0.0095\times 5\times 0.073 = 0.0035$ m^2

b) Total free flow area, $A_{ff} = \sigma \times A_{fr} = 0.8920\times 0.0035 = 0.002425$ m^2

c) Wall conduction area, $(a_w)_h = A_{fr} - A_{ff} = 0.0035 - 0.002425 = 0.001043$ m^2

Similarly, $(a_w)_c = 0.007213$ m^2

Therefore, Total wall conduction area (A_w) $= (a_w)_c + (a_w)_h = 0.00177$ m^2

d) Total heat transfer area, $A_h = \dfrac{4\times A_{ff}\times L}{D_e} = \dfrac{4\times 0.002425\times 0.9}{0.001673} = 5.215$ m^2

C. Input data for the test heat exchanger:

a) Hot fluid inlet temperature= 315 K

b) Cold fluid inlet temperature= 100K

c) $P_{hi}=P_{ci}$= 1.15 bar

d) $\dot{m}_h = \dot{m}_c$ = 10.5 gm/sec=0.0105 kg/sec

D. Fluid properties at mean temperatures:

The fluid properties at the assumed mean temperatures of 214.85K for the hot fluid and 196.375K for the cold fluid is achieved by using the GASPAK property package. The values of fluid properties are:

a) For hot fluid:

C_p = 1071 J/kgK

μ = 1.4421X 10^{-5} Pa-sec

Pr = 0.7198

K = 0.02163 W/mK

ρ = 1.55 Kg/m^3

b) For cold fluid:

C_p = 1101 J/kgK

μ = 1.2725 X 10^{-5} Pa-sec

Pr = 0.7252

K = 0.01933 W/mK

ρ = 1.82 Kg/m^3

E. Calculation of heat transfer coefficients and surface effectiveness of fins:

a) Mass velocity = $G = \frac{\dot{m}}{A_{ff}} = \frac{0.0105}{0.002425}$ = 4.33 kg/m^2-sec

b) Reynolds No. = Re $= \frac{GD_e}{\mu} = \frac{4.33 \times 0.001673}{1.4421 \times 10^{-6}}$ = 502.33

c) Now, $\mathrm{Re}* = 257 \times (l/s)^{1.23} (t/l)^{0.58} \frac{D_e}{[t + \frac{1.328l}{\mathrm{Re}^{0.5}}]}$

$= 257 \times (4.392) \times (0.1546) \times 5.064 = 755.132$

d) As Re<Re*:

The Colburn factor, j according to Joshi-Webb correlation is;

$j = 0.53 \times (\mathrm{Re})^{-0.5} (l/D_e)^{-0.15} (s/h)^{-0.14} = 0.53 \times 0.04155 \times 0.9161 \times 1.332 = 0.0293$

e) Convection heat transfer coefficient, $h = \frac{j \times C_p \times G}{\mathrm{Pr}^{0.667}} = \frac{0.02687 \times 1071 \times 4.33}{07198^{0.667}}$

=169.903 W/mK

f) Fin parameter, $\mathrm{M} = \sqrt{\frac{2 \times h}{k_f \times t}} = \sqrt{\frac{2 \times 179.172}{162 \times 0.0002}}$ = 102.195m^{-1}

g) Characteristic length of fins: as the hot layers are exposed more to the atmosphere, so the inner and outer layer height has to be taken.

For hot layers: height of fin in outer layer, $(l_h)_o$ = b= 0.0095m

Height of fin in inner layers, $(l_h)_i$ = b/2=0.00475m

For cold layers: Height of fin, (l_c) =b/2=0.00475m

h) Surface effectiveness of fin,

$(\eta_{fin})_{outer} = \frac{\tanh M (l_h)_o}{M (l_h)_o} = \frac{\tanh(105.166 \times 0.0095)}{105.166 \times 0.0095}$

=0.77

$(\eta_{fin})_{inner} = \frac{\tanh M (l_h)_i}{M (l_h)_i} = \frac{\tanh(105.166 \times 0.00475)}{105.166 \times 0.00475}$

=0.9282

i) Overall Surface effectiveness, $\eta_{oh} = 1 - \frac{a_f}{a_s}(1-\eta_{fi})[\frac{N_l - 2}{N_l}] - \frac{a_f}{a_s}(1-\eta_{fo})[\frac{2}{N_l}]$

=0.88

F. Overall heat transfer coefficient:

a) $\frac{1}{U_O A_O} = \frac{1}{(\eta_{oh} h_h A_h)} + \frac{a}{k_f A_w} + \frac{1}{(\eta_{oc} h_c A_c)} = 1.224\times10^{-3} + 7.51\times10^{6} + 2.1675\times10^{-3}$

=0.0035

$U_O A_O$ = 289.167 W/K

b) $U_{oh} = \frac{U_O A_O}{A_{oh}} = \frac{289.167}{5.215}$ =55.45 W/m^{2}K

$U_{oc} = \frac{U_O A_O}{A_{oc}} = \frac{289.167}{3.4524}$ =85.2265 W/m^{2}K

c) $NTU = \frac{U_O A_O}{C_{\min}} = \frac{289.167}{11.2455}$ =25.72

$C_{min}=C_h$=11.2455 J/K-sec

$C^*=C_{min}/C_{max}$=0.973

G. Effectiveness:

$$\varepsilon = \frac{1-e^{-NTU(1-C^*)}}{1-C^* e^{-NTU(1-C^*)}} = \frac{1-e^{-25.72\times0.027}}{1-0.973e^{-25.72\times0.027}} = 0.974$$

H. Effect of longitudinal conduction(Using Kroeger's equation):

a) Wall conduction area, A_w = 0.00177 m^2

b) Fin conductivity, K_f = 162 W/mK

c) Wall conduction parameter, $\lambda = \frac{k_f \times A_w}{L \times C_{\min}}$ =0.02833

d) $y = \lambda.NTU.C^* = 0.04833\times25.72\times0.973 = 0.709$

e) $\gamma = \frac{(1-C^*)}{(1+C^*)(1+y)} = \frac{0.027}{1.973 \times 1.709}$ =8.007 X 10^{-3}

f) $\phi = \left(\frac{y}{1+y}\right)^{0.5}\left[\frac{1+\gamma}{1/y - \gamma - \gamma^2}\right]$ =0.644 X 0.72=0.464

g) $\varphi = \frac{1+\gamma\phi}{1-\gamma\phi} = \frac{1+0.003715}{1-0.003715}$ = 1.00745

h) $r_1 = \frac{(1-C^*)NTU}{1+\lambda.NTU.C^*} = \frac{0.027 \times 25.72}{1+0.709}$ = 0.4063

i) Ineffectiveness, 1-ε = $= \frac{1-C^*}{\varphi e^{r_1} - C^*} = \frac{0.027}{1.51244 - 0.973}$ =0.05005

j) Efffectiveness(from Kroeger's equation) = 1-(1-ε) = 1-0.05005

=0.94995=0.95

I. The outlet temperature obtained from this effectiveness is;

a) For hot fluid, $T_{ho} = T_{hi} - \frac{\varepsilon C_{\min}(T_{hi} - T_{ci})}{C_h}$ = 112.7.65K

b) For cold fluid, $T_{co} = T_{ci} + \frac{\varepsilon C_{\min}(T_{hi} - T_{ci})}{C_c}$ = 296.78K

c) The mean temperatures for the respective outlet temperatures are, 213.85K and 198.40K which are in approximation with our assumed values.

J. Pressure drop:

a) Friction factor, $f = 8.12(\mathrm{Re})^{-0.74}(\frac{l}{D_e})^{-0.41}(\frac{s}{h})^{-0.02}$

= 0.08144 X 0.073 X 1.042

=0.06194

b) Pressure drop relation from Darcy-Weisbach relation is;

$\Delta P = \frac{4fLG^2}{2D_e\rho} = \frac{4 \times 0.06194 \times 0.9 \times 4.33^2}{2 \times 0.001673 \times 1.55}$ =806.10Pa

The calculation for the cold fluid follows the same fashion. Also the calculations using the other correlations of Maiti-Sarangi and Manglik- Bergles follows the same procedure. The results from calculations of the performance factors are given in tables- 5.2, 5.3 and 5.4.

Table 5-2 Results obtained from Joshi-Webb correlation

Factors	**Re no.**	**j**	**h(W/m^{2}K)**	**ε**	**f**	**ΔP(Pa)**
Hot Side	502.33	0.0293	169.903	0.95	0.06194	806.10
Cold Side	851.08	0.02068	141.053	0.95	0.04612	520.6332

Table 5-3 Results from Maiti-Sarangi correlation

Factors	**Re no.**	**j**	**h(W/m^{2}K)**	**ε**	**f**	**ΔP(Pa)**
Hot Side	502.3173	0.02201	127.10	0.941	0.075	971.83
Cold Side	851.08	0.01588	108.3135	0.941	0.05845	667.20

Table 5-4 Results from Manglik-Bergles correlation

Factors	**Re no.**	**j**	**h(W/m^{2}K)**	**ε**	**f**	**ΔP(Pa)**
Hot Side	495.805	0.024	114.424	0.9324	0.095	705
Cold Side	1420.715	.01872	110.8424	0.9324	0.04696	209.20

The following tables, table- 5.5, 5.6 and 5.7 shows the comparison of the various predicted values obtained of the effectiveness, effectiveness with Kroeger's equation, and pressure drop values for different correlations at a mass flow rate of 10.5 gm/sec and at temperatures between 315K to 100K.

Table 5-5 Calculated value of effectiveness using various correlations

Mass flow rate (kg/sec)	**Effectiveness**			
	Joshi-Webb	Manglik-Bergles	Maiti-Sarangi	Aspen MUSE
0.0105	0.978	0.9454	0.9635	0.895

Table 5-6 Calculated values of effectiveness using Kroeger's longitudinal wall heat conduction equation

Mass flow rate(kg/sec)	**Effectiveness(using Kroeger's equations)**			
	Joshi-Webb	Manglik-Bergles	Maiti-Sarangi	Aspen MUSE
0.0105	0.9508	0.9324	0.941	0.895

Table 5-7alculated values of pressure drop for various correlations

Mass flow rate (kg/sec)	**Pressure drop (Pa) max.**			
	Joshi-Webb	Manglik-Bergles	Maiti-Sarangi	Aspen MUSE
0.0105	806.20	705	971.83	502

CHAPTER-6

Results and discussions

6. RESULTS

The present investigation deals with the simulation of the test heat exchanger with cold layer test and hot layer test at different mass flow rates and at different cold fluid inlet temperatures and the evaluation of the thermal performance factors like effectiveness and pressure drops. In this chapter, the results obtained from the simulation are presented in the tabular form and also the comparison between the cold and hot layer test is shown with the help of graphs.

6.1 Simulation Results:

6.1.2 Simulation with Cold Layer Test:

Table 6-1 Results obtained at 80K

m	**ΔP_h**	**ΔP_c**	**T_{ho}**	**T_{hi}**	**T_{co}**	**T_{ci}**	**ε**
(gm/sec)	(Pa)	(Pa)	(K)	(K)	(K)	(K)	
5	162	167	112.95	315	286.47	80	0.859787
6	177	219	107.76	315	290.21	80	0.881872
7	193	274	107.46	315	291.85	80	0.883149
8	209	330	106.9	315	292.48	80	0.885532
9	227	391	106.53	315	292.96	80	0.887106
10	245	453	105.66	315	293.58	80	0.890809
12	283	593	105.81	315	293.81	80	0.89017
15	349	832	106.13	315	293.78	80	0.888809

Table 6-2 Results obtained at 90K

m	**ΔP_h**	**ΔP_c**	**T_{ho}**	**T_{hi}**	**T_{co}**	**T_{ci}**	**ε**
(gm/sec)	(Pa)	(Pa)	(K)	(K)	(K)	(K)	
5	161	176	115.82	315	291.28	90	0.885244
6	175	228	116.47	315	291.31	90	0.882356
7	192	285	115.5	315	293.55	90	0.886667
8	208	343	115.53	315	293.5	90	0.886533
9	226	405	115	315	293.8	90	0.888889
10	244	470	114.23	315	294.5	90	0.892311
12	282	614	114.32	315	294.72	90	0.891911
15	352	860	114.39	315	294.77	90	0.8916

Table 6-3 Results obtained at 100K

m	**ΔP_h**	**ΔP_c**	**T_{ho}**	**T_{hi}**	**T_{co}**	**T_{ci}**	**ε**
(gm/sec)	(Pa)	(Pa)	(K)	(K)	(K)	(K)	
5	157	184	129.26	315	289.31	100	0.863907
6	174	240	126.44	315	292.43	100	0.877023
7	191	297	124.13	315	295.02	100	0.887767
8	208	356	123.95	315	294.62	100	0.888605
9	226	423	123.31	315	295.71	100	0.891581
10	245	487	122.86	315	295.47	100	0.893674
12	286	636	122.96	315	295.65	100	0.893209
15	355	889	122.92	315	295.75	100	0.893395

Table 6-4 Results obtained at 110K

m	**ΔP_h**	**ΔP_c**	**T_{ho}**	**T_{hi}**	**T_{co}**	**T_{ci}**	**ε**
(gm/sec)	(Pa)	(Pa)	(K)	(K)	(K)	(K)	
5	168	256	131.65	315	292.59	110	0.88127
6	176	268	133.94	315	293.42	110	0.88322
7	190	308	132.6	315	296.02	110	0.889756
8	208	368	132.57	315	295.5	110	0.889902
9	227	438	131.74	315	296.73	110	0.893951
10	246	504	131.7	315	296.3	110	0.894146
12	266	578	131.34	315	296.61	110	0.895902
15	288	657	131.52	315	296.55	110	0.895024

6.2 Simulation with Hot Layer Test:

Table 6-5 Results obtained at 80K

m	**ΔP_h**	**ΔP_c**	**T_{ho}**	**T_{hi}**	**T_{co}**	**T_{ci}**	**ε**
(gm/sec)	(Pa)	(Pa)	(K)	(K)	(K)	(K)	
5	180	127	111.56	315	288.09	80	0.865702
6	200	163	107.72	315	291.05	80	0.882043
7	222	201	107.25	315	292.09	80	0.884043
8	244	241	106.69	315	292.71	80	0.886426
9	268	283	105.9	315	293.25	80	0.889787
10	293	328	105.5	315	293.79	80	0.891489
12	348	426	105.63	315	294.03	80	0.890936
15	442	591	105.95	315	293.99	80	0.889574

Table 6-6 Results obtained at 90K

m	**ΔP_h**	**ΔP_c**	**T_{ho}**	**T_{hi}**	**T_{co}**	**T_{ci}**	**ε**
(gm/sec)	(Pa)	(Pa)	(K)	(K)	(K)	(K)	
5	179	135	118.72	315	290.57	90	0.872356
6	199	170	116.36	315	292.21	90	0.882844
7	221	210	115.31	315	293.79	90	0.887511
8	244	251	115.23	315	293.72	90	0.887867
9	270	298	114.3	315	295.15	90	0.892
10	294	341	114.07	315	29407	90	0.893022
12	351	442	114.13	315	294.93	90	0.892756
15	448	611	114.21	315	294.97	90	0.8924

Table 6-7 Results obtained at 100K

m	**ΔP_h**	**ΔP_c**	**T_{ho}**	**T_{hi}**	**T_{co}**	**T_{ci}**	**ε**
(gm/sec)	(Pa)	(Pa)	(K)	(K)	(K)	(K)	
5	177	138	127.98	315	290.56	100	0.86986
6	199	177	125.98	315	292.96	100	0.879163
7	221	219	123.93	315	295.25	100	0.888698
8	245	261	123.89	315	294.7	100	0.888884
9	271	309	123.07	315	295.97	100	0.892698
10	296	354	122.72	315	295.65	100	0.894326
12	354	458	122.79	315	295.84	100	0.894
15	454	633	122.75	315	295.94	100	0.894186

Table 6-8 Results obtained at 110K

m	**ΔP_h**	**ΔP_c**	**T_{ho}**	**T_{hi}**	**T_{co}**	**T_{ci}**	**ε**
(gm/sec)	(Pa)	(Pa)	(K)	(K)	(K)	(K)	
5	177	144	136.47	315	291.79	110	0.870878
6	199	184	134.57	315	293.44	110	0.880146
7	222	257	132.4	315	296.23	110	0.890732
8	246	270	132.9	315	295.68	110	0.888293
9	272	320	131.52	315	296.95	110	0.895024
10	299	367	131.56	315	296.45	110	0.894829
12	354	474	131.36	315	296.77	110	0.895805
15	460	654	131.26	315	296.89	110	0.896293

6.2 Comparison between Cold layer test and Hot layer test:

6.2.1 Comparison between pressure drop values for Cold layer test and Hot layer test:

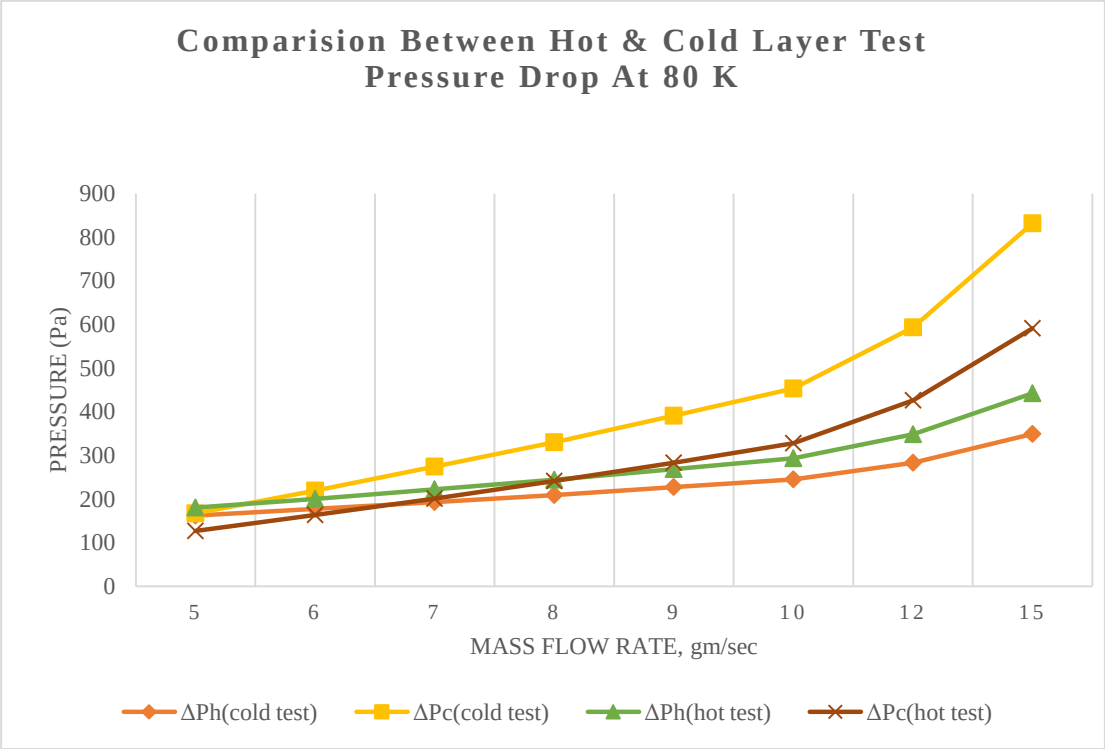

Figure 6.1 Pressure drop comparison at 80K

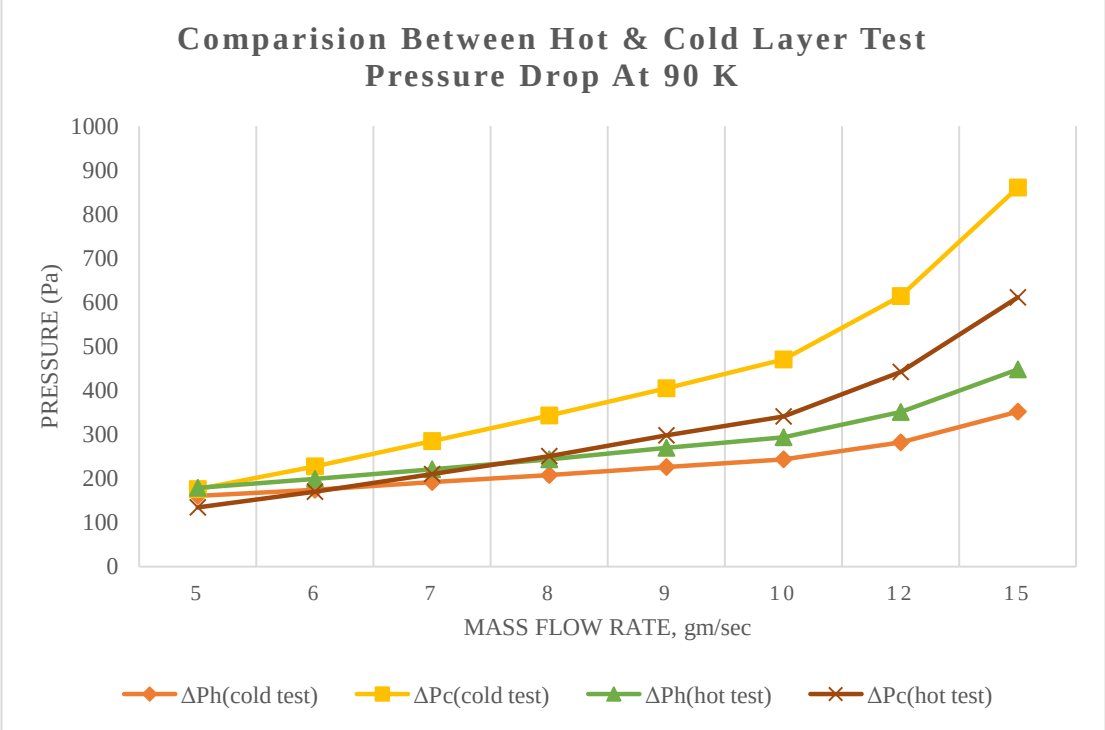

Figure 6.2 Pressure drop comparison at 90K

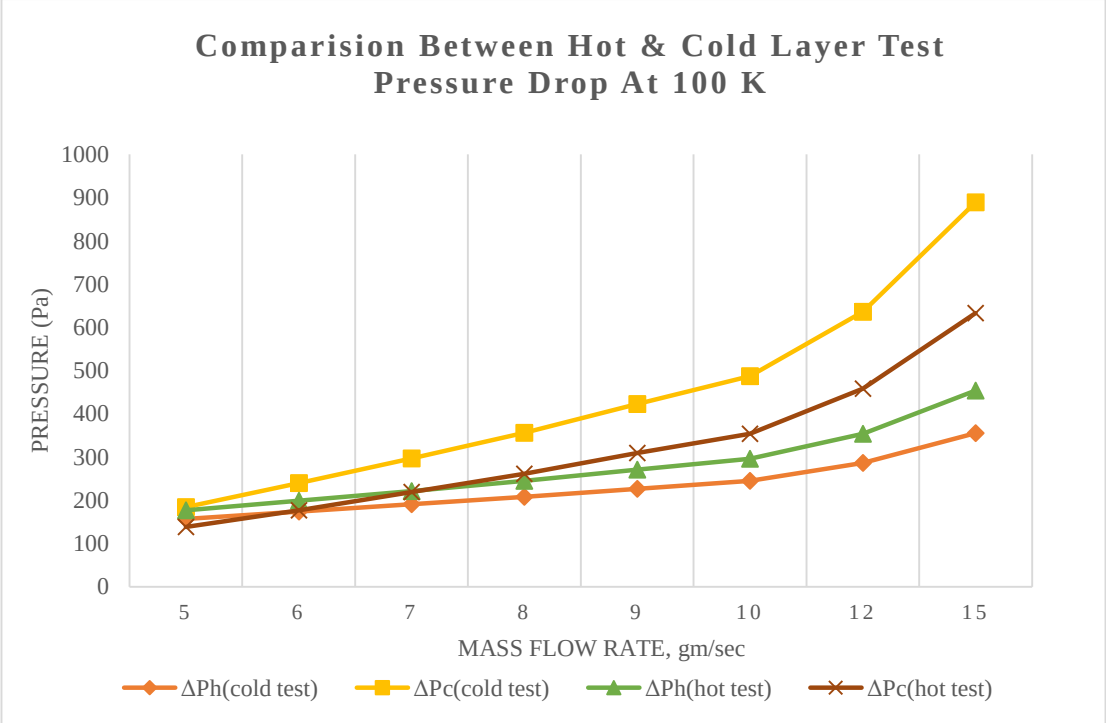

Figure 6.3 Pressure drop comparison at 100K

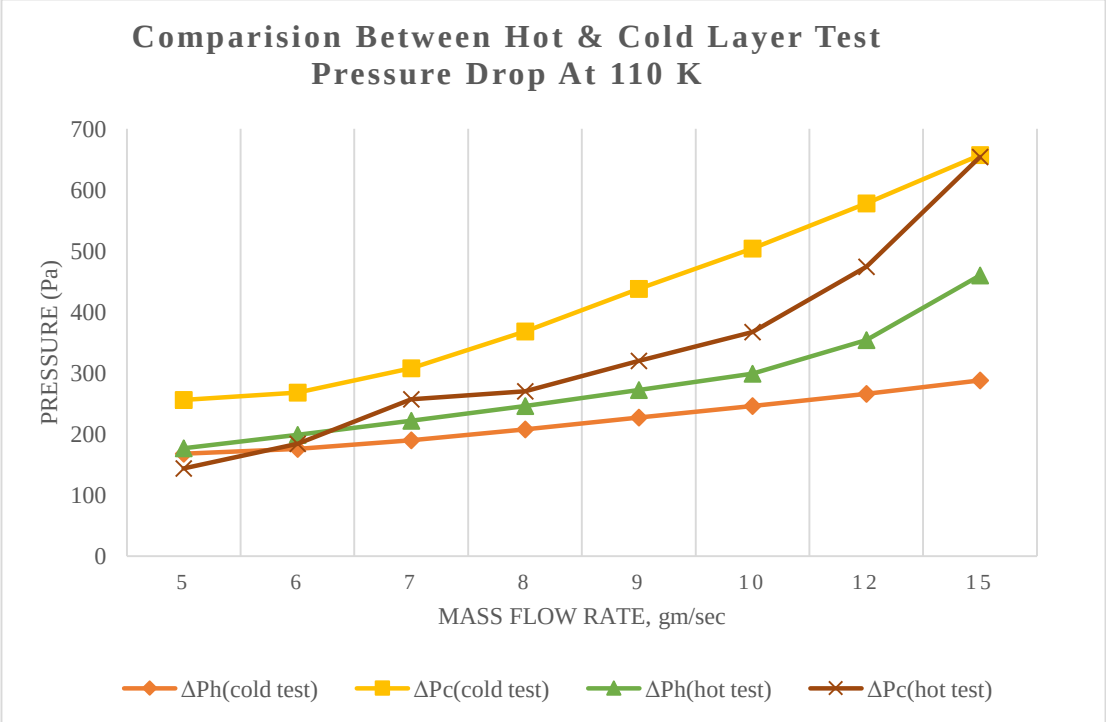

Figure 6.4 Pressure drop comparison at 110K

The above comparison graphs show that:

- The pressure drop of cold fluid for the cold layer tests is comparatively more than that for the hot layer test for all temperatures.

- In the same context, the pressure drop of hot fluid for the hot layer test is more than that for the cold layer test.

6.2.2 Comparison between effectiveness values for Cold layer test and Hot layer test:

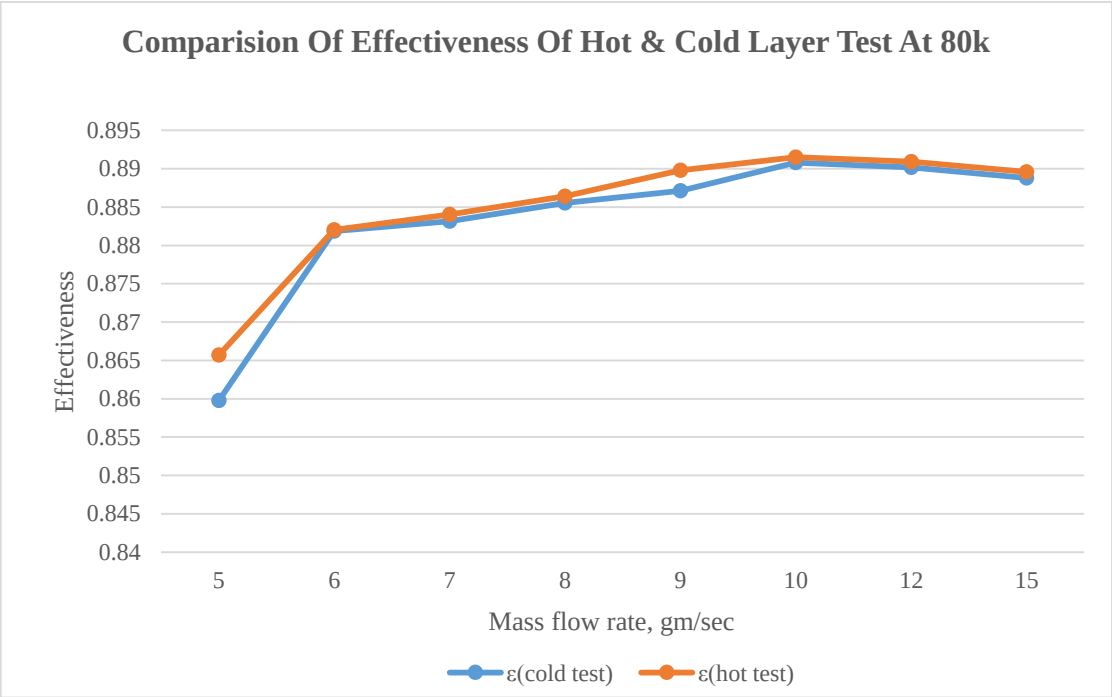

Figure 6.5 Effectiveness comparison at 80K

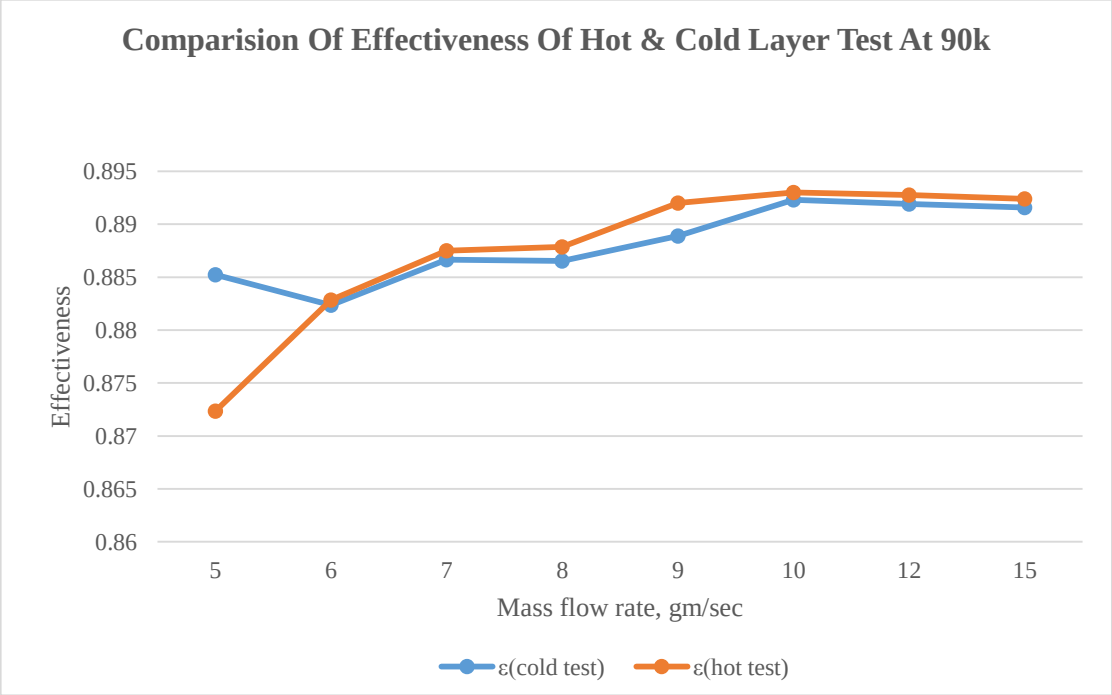

Figure 6.6 Effectiveness comparison at 90K

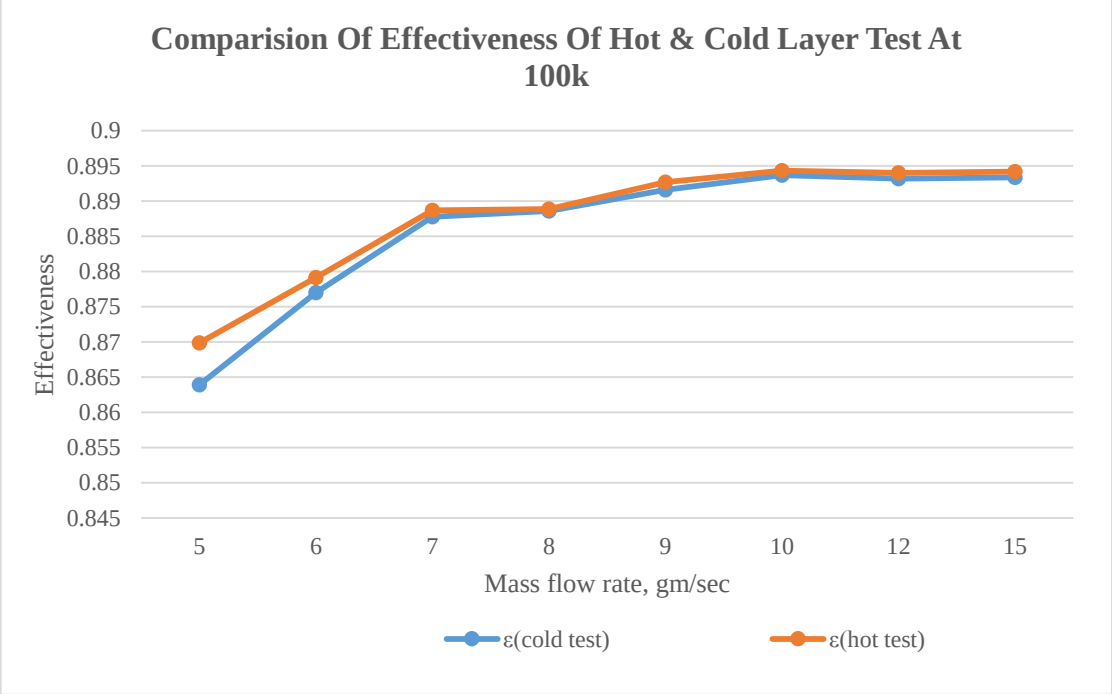

Figure 6.7 Effectiveness comparison at 100K

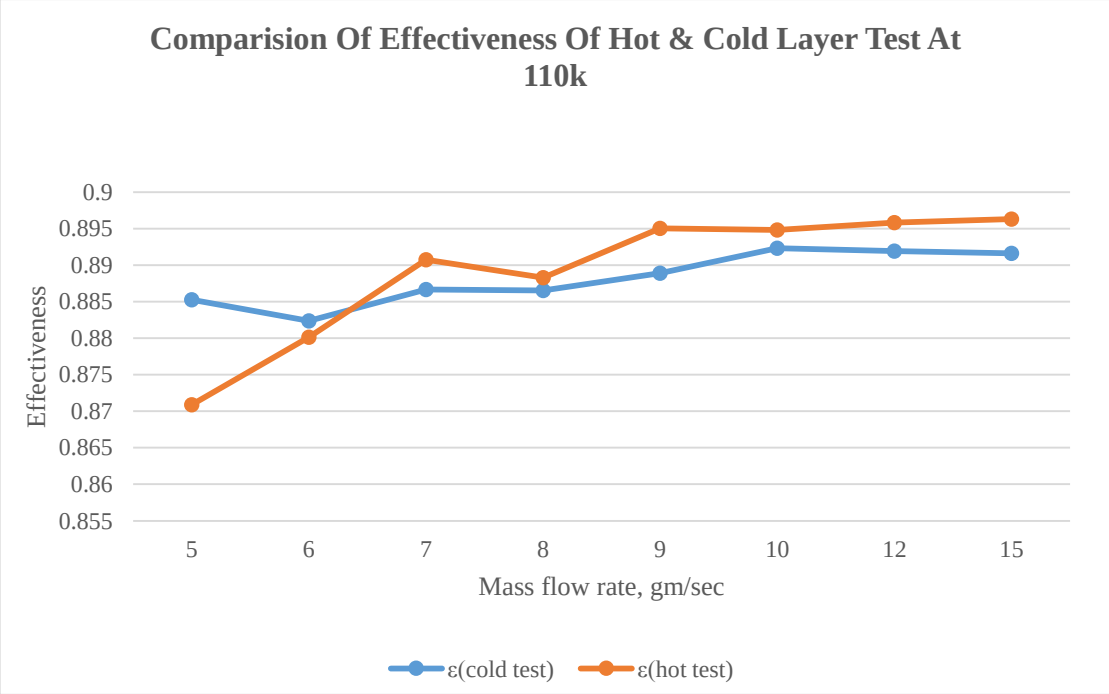

Figure 6.8 Effectiveness comparison at 110K

The above comparison graphs show that:

- The effectiveness for both the layer test shows similarity at all temperatures and mass flow rates.
- The effectiveness in between the mass flow rates of 5 gm/sec and 6 gm/sec shows absurd behaviour, i.e. does not match with the rest of the trend even after steady state.
- This is because of that at a particular temperature there is a mass flow rate at which the divergence ceases and we shall get normal results
- This particular mass flow rate can be the inlet mass flow rate of the fluid for that temperature at which experiment can be started.

CHAPTER- 7

Conclusion

7. CONCLUSION

The simulation of the test plate fin heat exchanger by the software Aspen MUSE [3] was carried out using the cold layer test method to actuate the performance factors like effectiveness and pressure drop and then using the rating procedure, the performance factors was also compared with the different correlations at different mass flow rates and inlet cold fluid temperatures and at single inlet hot fluid temperature of 315K.

The rating of the test heat exchanger at the mass flow rate of 10.5 gm/sec was done and the results compared with each other.

The concluding remarks are as follows;

- The percentage deviation between the results obtained from Joshi and Webb [24] correlation and with Aspen MUSE [3] simulation was found out to be 6.235%, whereas the deviation with that of Maiti and Sarangi [25]correlation is about 5.14% and with that of Manglik and Bergles [19] is about 4.18%.
- There is an under-prediction of the pressure drop by the various correlations and also by Aspen in relevance to the actual working conditions.
- The average effectiveness of the test plate fin heat exchanger is found to be 0.892.
- The simulation also shows that the effectiveness is increasing for increasing mass flow rates at all the specified inlet cold fluid temperatures.
- The fin efficiency is decreasing with the increasing temperature across the length of the exchanger for both the hot and cold fluids.
- The pressure drop is found to be increasing with increasing mass flow rate.
- It is found that at each of the inlet cold temperature there is a particular mass flow rate at which divergence ceases and we get a steady state solution. Thus the mass flow rate to be used for experimentation must be in this range to obtain results.

Table 7-1 Convergence occurance values

Sl. No.	**Mass flow rate(gm/sec)**	**T_{hi}**	**T_{ci}**
1	5.52	315	80
2	4.81	315	90
3	5.20	315	100
4	5.10	315	110

- The comparison between cold and hot layer test reveals that the pressure drop ranges for cold test method is higher than that for the hot test at all temperatures and the graphs for effectiveness shows that for low mass flow rates there is a deviation in the values of effectiveness occurring due to the divergence of results.

7.1 Scope for Future Work:

- To validate the values achieved from distinct correlations of effectiveness, overall heat transfer coefficient, etc., with the values obtained from the simulation software Aspen Muse [3] and integrate it with Aspen Hysys by experimentation.
- Comparison of the performance factors like heat transfer coeffeicient, effectiveness and pressure drop of the cold and hot layered tests with that obtained from experiments at the cryogenic temperatures of 80K-110K.

References

8. REFERENCES

[1] M. Khoshvaght-Aliabadi, F. Hormozi and A. Zamzamia, "Role of channel shape on performance of plate-fin heat exchangers:Experimental assessment," *International Journal of Thermal Sciences*, no. 79, pp. 183-193, 2014.

[2] S. Alur, "Experimental studies on plate fin heat exchangers," PhD Dissertation, National Institute of Technology Rourkela, 2009.

[3] A. Inc., "Aspen Muse Reference guide," Cambridge, Massachusetts, 2013.

[4] W. M. Kays and A. L. London, Compact Heat exchangers, McGraw-Hill, New York, 1984.

[5] R. K. Shah, P. Dusan and D. P. Sekulic, Fundamentals of Heat Exchanger Design, John Wiley & Sons,, 2003.

[6] J. E. Hesselgreaves, Compact Heat Exchangers; Selection, Design and Operation, Pergamon, 2001.

[7] T. Cowel and N. Achaichia, Compact Heat Exchangers in the Automobile Industry, Proceedings of the International Conference on Compact Heat Exchangers in the Process Industries, 1997.

[8] A. L. London and R. K. Shah, Offset Rectangular Plate –fin surfaces-Heat Transfer and Flow Friction Characteristics, Transactions of the ASME,Journal of Engineering for Power, 1968.

[9] A. M. Jacobi and R. K. Shah, Air Side Flow and Heat transfer in Compact Heat Exchangers: A Discussion of Enhancement Mechanisms, vol. 19(8), Heat Transfer Engineering, 1998, pp. 29-41.

[10] J. Dong, J. Chen and Z. Chen, Flow and heat transfer in compact offset strip fin surfaces, Higher Education Press and Springer-Verlag, 2008.

[11] S. V. Patankar, E. M. Sparrow and C. H. Liu, Fully Developed Flow and Heat Transfer in Ducts Having Stream wise-Periodic Variations of Cross-Sectional Area, Transactions of the ASME Journal of Heat Transfer, 1977, pp. 180-186.

[12] I. Ghosh, Experimental and Computational Studies on Plate Fin Heat Exchanger, PhD Dissertation, Indian Institute of Technology, Kharagpur, 2004.

[13] M. D. Paepe, A. Willems and A. Zenner, Experimental Determination of the Heat Transfer Coefficient of a Plate-Fin Heat Exchanger, Heat Transfer Engineering, 26(7), 2005, pp. 29-35.

[14] E. V. Dubrovsky, Experimental Investigation of Highly Effective Plate-Fin Heat Exchanger Surfaces, ELSEVIER, 1994.

[15] S. V. Patankar and C. Prakash, An Analysis of the Effect of Plate Thickness on Laminar Flow and Heat Transfer in Interrupted–plate passages, International Journal of Heat and Mass Transfer, 1981.

[16] K. Suzuki, E. Hirai and T. Miyake, Numerical and Experimental Studies on a Two-dimensional Model of an Offset-strip-fin Type Compact Heat Exchanger Used at Low Reynolds Number, International Journal of Heat and Mass Transfer, 1985.

[17] L. W. Zhang, D. K. Tafti, F. M. Najjar and S. Balachandar, "Computations of Flow and Heat Transfer in Parallel-Plate Fin Heat Exchangers on the CM-5: Effects of Flow Unsteadiness and Three-Dimensionality," *International Journal of Heat and Mass Transfer*, 1997.

[18] R. K. Shah, L. S. Ismail and C. Ranganayakulu, "Numerical study of flow patterns of compact plate-fin heat exchangers," *International Journal of Heat and Mass Transfer,* no. 52, p. 3972–3983, 2009.

[19] R. M. Manglik and A. E. Bergles, "Heat Transfer and Pressure Drop Correlations For the Rectangular Offset strip Fin Compact Heat Exchanger," *Experimental Thermal and Fluid Science,* no. 10, pp. 171-180, 1995.

[20] S. V. Manson, "Correlation of Heat Transfer Data and of friction Data for Interrupted Plane fins Staggered in Successive rows," NACA Tech. Note 2237, National Advisory Committee for Aeronautics, Washington, DC, 1950.

[21] W. M. Kays, "Compact Heat Exchangers," AGARD lecture Serr. No 57 on Heat exchangers, AGARD-LS-57-72, NATO, paris, 1972.

[22] F. V. Tinaut, A. Melgar and A. A. Rehman Ali, "Correlations for Heat Transfer and FlowFriction Characteristics of Compact Plate Type Heat Exchangers," *International Journal of Heat,* 1992.

[23] A. R. Weiting, "Empirical Correlations for Heat Transfer and Flow Friction Characteristics of Rectangular Offset-fin Plate-fin Heat Exchangers," *ASME Journal of Heat Transfer*, no. 97, pp. 488-490., 1975.

[24] H. M. Joshi and R. L. Webb, "Heat Transfer and Friction in the Offset Strip-fin Heat Exchanger," *International Journal of Heat and Mass Transfer,* no. 30 (1), pp. 69-84, 1987.

[25] D. K. Maiti and S. K. Sarangi, "Heat Transfer and Flow Friction Characteristics of Plate Fin Heat Exchanger Surfaces- A Numerical Study," PhD Dissertation, Indian Institute of Technology, Kharagpur, Kharagpur, 2002.

[26] R. F. Barron, Cryogenic systems, Oxford University Press, 1985.

[27] P. G. Kroeger, "Performance deterioration in high effectiveness heat exchanger due to Axial Conduction Effect," *Advances in Cryogenic Engineering,* vol. 12, no. 8, pp. 363-372, 1966.

[28] G. Venkatarathnam and S. P. Narayanan, "Performance of a counter flow heat exchanger with longitudinal heat conduction through the wall separating the fluid streams from the environment," *Cryogenics,* no. 39, pp. 811-819, 1999.

[29] M. D. Atrey and P. Gupta, "Performance evaluation of counter flow heat exchangers considering the effect of heat in leak and longitudinal conduction for low-temperature applications," *Cryogenics,* vol. 7, no. 40, pp. 469-474, 2000.

[30] P. Gupta, P. K. Kush and M. D. Atrey, "Numerical simulation and experimental inverstigation of tube-in-tube cryogenic counter flow heat exchangers," in *ICEC-18,* 2000.

[31] H. Peng and X. Ling, "Optimal design approach for the plate-fin heat exchangers usingneural networks cooperated with genetic algorithms," *Applied Thermal Engineering,* no. 28, pp. 642-650, 2008.